

Plasmoids in Reconnecting Current Sheets: Solar and Terrestrial Contexts Compared

J. Lin,^{1, 2} S. R. Cranmer,² C. J. Farrugia³

Abstract. Magnetic reconnection plays a crucial role in violent energy conversion occurring in the environments of high electrical conductivity, such as the solar atmosphere, magnetosphere, and fusion devices. We focus on the morphological features of the process in two different environments, the solar atmosphere and the geomagnetic tail. In addition to indirect evidence that indicates reconnection in progress or having just taken place, such as auroral manifestations in the magnetosphere and the flare loop system in the solar atmosphere, more direct evidence of reconnection in the solar and terrestrial environments is being collected. Such evidence includes the reconnection inflow near the reconnecting current sheet, and the outflow along the sheet characterized by a sequence of plasmoids. Both turbulent and unsteady Petschek-type reconnection processes could account for the observations. We also discuss other relevant observational consequences of both mechanisms in these two settings. While on face value, these are two completely different physical environments, there emerge many commonalities, for example, an Alfvén speed of the same order of magnitude, a key parameter determining the reconnection rate. This comparative study is meant as a contribution to current efforts aimed at isolating similarities in processes occurring in very different contexts in the heliosphere, and even in the universe.

1. Introduction

Magnetic reconnection is one of the fundamental physical processes that occur in magnetized plasmas, and manifestations range from laboratory to magnetospheric plasmas, and to solar and astrophysical plasmas. Reconnection has as its main characteristic feature the conversion of magnetic field energy into other forms of energy, and transfer of plasma and magnetic flux between separate flux systems: a re-arrangement of magnetic topology. This process is associated with phenomena such as heating of the solar corona, solar eruptions, coupling between the solar wind and the terrestrial magnetosphere, substorms in the geomagnetic tail, and on a more speculative level, high-energy phenomena observed in astrophysical systems [e.g., see *Priest and Forbes 2000*].

Because these phenomena occur in environments of high electrical conductivity, the energy conversion process is usually confined to a small, local region, such as the X-type neutral point, the current sheet, the quasi-separatrix layer, and so on. Among these types of magnetic neutral regions, the X-point is probably the most basic configuration from which the others could develop. For example, a current sheet could develop either through the collapse of an X-point [*Dungey 1953*] or through the severe stretching of the magnetic field around an X-point [*Forbes and Isenberg 1991*]; and a quasi-separatrix layer [*Démoulin et al. 1996*] might be produced by skewing the magnetic fields on both sides of an X-point.

At the current sheet separating the shocked solar wind and the terrestrial magnetosphere (the magnetopause), magnetic reconnection can transfer solar wind momentum and energy into the magnetosphere on the dayside. Figure 1 displays a schematic of the topological changes that are initiated by magnetic reconnection between solar wind field and terrestrial field on the dayside (stage 1). Reconnected (or “open”) field lines are then dragged by the shocked solar wind flow into the nightside magnetosphere, where they form the tail lobes (stage 2). Addition of magnetic flux from the dayside to the nightside increases the energy stored in the tail. A thin current sheet forms in the tail and at substorm onset reconnection takes place there (stage 3), heating plasma and jetting it in bursty fashion both earthward [*Baumjohann et al., 1990; Angelopoulos et al., 1992*] (stage 4) and tailward (stage 5) at high speeds. On the earthward side, reconnected field lines rapidly snap back toward the Earth due to magnetic tension, constituting a process known as the shrinkage of field lines [e.g., see *Švestka et al. 1987; Lin et al. 1995a; Forbes and Acton 1996; Lin 2004; Reeves et al. 2008*]. These field lines eventually return to the dayside and replace the eroded magnetic flux.

Magnetic reconnection and a general convective cycle, including frontside and nightside reconnections, in the process described above were proposed for the first time by *Dungey [1961]*. Later, the substorm model was developed, particularly by *McPherron et al. [1973]*, *Hones [1977]*, and *McPherron [1991]*. (See also *Baker et al. [1996]* for a more recent review.) As emerges from the discussions above, the substorm is an explosive energy release and is accompanied by a reconfiguration of the near-tail magnetic field (dipolarization) and other phenomena to be discussed later. If the magnetosphere is immersed in a southward-pointing interplanetary magnetic field of long (many hours) duration, such as what typically happens during passage of interplanetary coronal mass ejections (ICMEs), then repetitive substorms [*Farrugia et al. 1993a*] occur at intervals of about 2–3 hours [*Huang et al. 2003*].

The formation and development of a current sheet and/or a quasi-separatrix in the solar magnetic field is usually associated with solar eruptive processes, including solar flares,

¹National Astronomical Observatories of China/Yunnan Astronomical Observatory, Chinese Academy of Sciences, Kunming, Yunnan 650011, China

²Harvard-Smithsonian Center for Astrophysics, 60 Garden Street, Cambridge, MA 02138, USA.

³Institute for the Study of Earth, Ocean, and Space, University of New Hampshire, Durham, NH 03824, USA.

eruptive prominences, and coronal mass ejections (CMEs). In fact, substorms have been called the flares in the magnetosphere; i.e., loosely speaking, due to the similarity and explosive character in the energy conversion processes, substorms may be considered as the magnetospheric counterparts of solar eruptions. As we show below, a comparison of reconnection in the solar and terrestrial contexts reveals many common features.

Table 1 lists some important parameters for the solar atmosphere and for the magnetosphere. Those for the solar atmosphere can be found in the book by *Priest* [1982], those for the low latitude dayside magnetosphere were taken from the *in situ* measurements reported by *Paschmann et al.* [1986], those for the middle distant tail lobe and the plasma sheet are from *Slavin et al.* [1985], and those for the near Earth sheet are from *Baumjohann et al.* [1989]. We notice the same orders of magnitude of large V_A and small β in the solar corona and in the tail lobes of the magnetosphere, but small V_A and larger β in the solar photosphere, in the dayside magnetopause, and in the central plasma sheet in the geomagnetic tail. Those in the central sheet (e.g., see *Baumjohann et al.* [1989]) suggest a rapid increase of the reconnection rate when low density, high Alfvén speed, lobe field becomes reconnected (e.g., *Hesse et al.* [1996]). However, the corresponding values for the solar counterpart of the geomagnetic tail sheet are not available due to the lack of *in situ* measurements in the solar environment. On the other hand, the low V_A and high β in the solar photosphere and in the dayside magnetopause have different consequences that will be discussed shortly.

So even though Table 1 indicates some similarities of the current sheet in the magnetosphere to that in the solar corona, the levels of our understanding of the details of magnetic reconnection in the magnetosphere and in the solar corona are very disparate. In the magnetosphere, extensive *in situ* measurements reveal tremendously rich information of the internal features of the current sheets and the magnetic reconnection processes at the magnetopause (e.g., *Rijnbeek et al.* [1989]; *Sonnerup et al.* [1981]; *Phan et al.* [2000]; *Paschmann* [2005]), and in the magnetotail (e.g., *Murata et al.* 1995; *Baker et al.* 1985; *Nakamura et al.* 2006). In the solar corona, on the other hand, directly observing the current sheet turns out to be very hard, if not impossible. Difficulties stem from two aspects: the low level of emission from the sheet plasma compared to that of other nearby bright features (see the introduction of *Ko et al.* [2003] for a brief review), and the possible thinness of the sheet.

In theory, it has often been stated that the sheet is too thin to be observable since its thickness is believed to be limited by the Larmor radius of particles that is only a few tens of meters in the coronal environment [*Litvinenko* 1996; *Wood and Neukirch* 2005; and references therein]. Another reason that might have discouraged direct observations of the current sheet could be ascribed to the “circuit model” of eruptions developed by *Martens and Kuin* [1989], in which the theoretical current sheet length is short. Not until the theoretical works of *Forbes and Lin* [2000], *Lin and Forbes* [2000], and *Lin* [2002], as well as a series subsequent observational ones [*Ciaravella et al.* 2002; *Ko et al.* 2003; *Raymond et al.* 2003; *Sui and Holman* 2004; *Sui et al.* 2004; *Webb et al.* 2003; *Lin et al.* 2005; *Bemporad et al.* 2006; *Lin et al.* 2007], have we started realizing that a fairly long current sheet could develop in the major eruptive process.

In this work we undertake a comparison of the reconnection processes in these two environments, putting emphasis on geomagnetic substorms, on the one hand, and solar flares, on the other. Such a comparison consists of two aspects. First, we look into the detailed internal structures of the reconnecting sheets observed in the geomagnetic environment and in the solar corona; second, we compare two theoretical mechanisms that may account for the observed features of the reconnecting current sheet. This brings the known results for magnetic reconnection obtained from the investigations of various communities together, and helps people of different research areas to better understand the work and the progress made by others.

2. Reconnection-related plasmoids (plasma blobs) in the solar and terrestrial environments

In this part of work, we go through a set of observational results regarding plasmoids (plasma blobs) observed in different environments. The term “plasmoid” is usually used to describe flowing features in the geomagnetic tail current sheet [e.g., see *Murata et al.* 1995 and references therein]. The term “plasma blob”, on the other hand, is used for the similar features observed in the CME/flare sheets [see *Ko et al.* 2003]. Observed morphological features and the possible causative mechanisms suggest that plasma blobs and plasmoids are likely the same object, produced by reconnection.

2.1. Reconnection Processes Observed in the Magnetotail

The existence of the Earth’s geomagnetic tail and its embedded current sheet was confirmed by extensive *in situ* measurements of the magnetic field of the Earth at distances greater than 7 Earth radii in the 1960s [e.g. see *Ness* 1965], and has been observed hundreds of Earth radii from the Earth by spacecraft. The discovery of the neutral sheet in the magnetotail is an important aspect in determining the interaction of the super Alfvénic solar wind with the Earth’s magnetic field. The dynamics of this sheet may thus play an essential role in geomagnetic phenomena [*Ness* 1965]. The geomagnetic tail consists of magnetized plasma in the tail lobes overlaying the plasma sheet, in which the current sheet is embedded separating two oppositely-directed magnetic fields. The geomagnetic tail results from the flow of the solar wind around the magnetosphere. Reconnection of the magnetospheric and the interplanetary magnetic fields starts on the dayside. Open flux is transferred to the nightside where it is stored during the substorm growth phase until released again to the dayside at the substorm onset (see also Figure 1 for the cycle).

Dayside reconnection may be quasi-steady [e.g., *Sonnerup et al.* 1981] or time-dependent. The latter form was discovered by *Russell and Elphic* [1978] at about the same time as observational evidence was being shown for steady reconnection. Time dependent reconnection features on the dayside are known as flux transfer events (FTEs). These are tied to various signatures, chief among these is a bipolar variation lasting 1-2 min of the magnetic field component normal to the magnetopause (see reviews by *Elphic* [1995] and *Farrugia et al.* [1988]). The low V_A and high β in this region (see Table 1) imposes restrictions on the rate of magnetic reconnection and thus the energy conversion. So particle acceleration and plasma heating at the dayside magnetopause are not as obvious as in the tail region *Cowley* [1980]. Instead reconnection here primarily leads to the storage of magnetic reconnection converted from the solar wind kinetic energy (see Figure 1).

As indicated by Figure 1, after reconnection on the dayside open field lines are dragged to the nightside forming the tail lobes. This results in a considerable increase in the energy stored in the tail. To balance the dayside reconnection during relatively quiet times, nightside reconnection is needed, which is assumed to take place in the far tail forming the quiet time plasma sheet. During the rapid accretion of magnetic energy in the tail lobe during disturbed conditions, however, the plasma sheet closer to Earth (at

10 – 20 Re) becomes thinner. When it becomes sufficiently thin, a near-Earth neutral line is created. At the neutral line plasma is heated and jets in both earthward and tailward directions. In earthward direction, closer to the Earth than the neutral sheet the field lines become more dipolar through magnetic tension, injecting energetic particles near local midnight in the process. Strong auroral effects are produced at the magnetic footprints of these field lines (e.g. *Sergeev et al.* [1999]; *Sandholt et al.* [2001]); and in the tailward direction, a “magnetic island” or plasmoid is propelled at high speeds.

The term “plasmoid” was first introduced by *Hones et al.* [1977] who took it from the laboratory literature where the pulse of plasma emitted into a chamber to conduct experiments was termed a plasmoid. Magnetotail plasmoids as regions of typically reduced magnetic field strength (except when they contain a strong core field), surrounded by a traveling compression region, were discovered in the ISEE data in the mid-1980s [*Hones et al.* 1984; *Slavin et al.* 1984]. They are large (about tens of Re) closed magnetic loops which propagate rapidly downtail during a substorm event [*Hones et al.* 1984]. *Slavin et al.* [1984] described traveling convection regions observed by ISEE in the distant tail consequent upon substorm activity nearer Earth and identified them as lobe signatures of plasmoids traveling at a few 10^2 km s^{-1} downtail. The release of plasmoids in the near-Earth tail at substorm expansion phase was inferred by *Hones* [1979].

Features of the distant neutral line (DNL) are also summarized in Figure 1. The DNL was first demonstrated with actual measurements from ISEE 3 by *Slavin et al.* [1985]. It was then examined in a series of further studies using Geotail data by *Nishida et al.* [1994; 1998; and references therein]. Reconnection at the DNL appears relatively continuous and moderate in terms of its outflow speed, perhaps due to the fact that the lobes are filled with diffuse plasma by x (GSM) $\sim 100Re$ from the “mantle” that lowers the Alfvén speed.

Magnetic island structures in the magnetotail have been frequently detected by *in situ* measurements either by direct encounter or by remote sensing the perturbations they excite in the surrounding field and plasma [*Slavin et al.* 1984] during geomagnetic substorms, and the flow speed could be as high as several hundreds of km/s [*Ho and Tsurutani* 1997]. Reports in a series of recent works on the multiple X-line reconnection (e.g., *Slavin et al.* [2003]; *Slavin et al.* [2005]; and *Eastwood et al.* [2005]) based on the observations made by the four Cluster spacecrafts confirmed the magnetic island structure inside the current sheet. These observations indicated the occurrence of the multiple X-line reconnection in the magnetotail proposed by *Lee and Fu* [1985] and *Fu and Lee* [1985].

These authors found plasmoid features moving both earthward and tailward, and argued that they are the products of the multiple X-line reconnection. The rate of reconnection at each X-line is not necessarily the same. Instead, one of these X-lines becomes dominant where the fastest reconnection takes place. *Eastwood et al.* [2005] pointed out that although numerical and experimental evidence had been observed to suggest the filamentation of the current sheet and multiple X-line reconnection, the data from Cluster and related investigations presented the observational evidence of the relevant features in the magnetotail for the first time. On the other hand, what determines the location of the dominant X-line is unknown. It probably depends on the adjacent magnetic field and the plasma environment.

Some other interesting characteristics of plasmoids are that plasmoids observed to move tailward are more than those moving earthward [*Moldwin and Hughes* 1991], and that the tailward motion is faster than the earthward motion [*Slavin et al.* 2003]. This is probably due to the fact that the earthward flow is deflected and stopped near the

cusplike point by the closed magnetic field lines near the Earth, as described by *Reeves et al.* [2008] in a recent work related to the present one. Because of mathematical complexity, the behavior of the plasmoid approaching the cusplike region was tentatively studied via the analytic approach in only two works so far [i.e., *Semenov and Lebedeva* 1991; *Lin et al.* 1995b], and no numerical experiment focusing on the behavior of the plasmoid near that area has yet been reported.

Another important consequence of reconnection is the generation of fast plasma flows, which for a long time have been used as the major indicator of the occurrence of reconnection and for the identification of the location of the reconnection site. On the dayside, accelerated plasma flows have been extensively used to infer the presence of reconnection [see *Paschmann et al.* 1979; *Sonnerup et al.* 1981] in view of the difficulty in showing a non-zero normal component. In the tail, bulk plasma acceleration associated with the formation of the slow mode shock that has been identified (e.g., see *Feldman et al.* [1984]; *Øieroset et al.* [2000]; and *Sonnerup et al.* [1987]) implicitly suggests that the Petschek-type reconnection is in operation. Large-scale hybrid simulations of the magnetotail undergoing reconnection were conducted, and significance of the slow mode shocks was confirmed [*Krauss-Varban and Omid* 1995]. But in the quasi-steady state framework, not all the observed and simulated features, such as the slow mode shock, gave a coherent and consistent picture [*Feldman et al.* 1985; *Krauss-Varban and Omid* 1995]. From this time-dependent properties of reconnection process in reality may be inferred [e.g., *Pudovkin and Semenov* 1985].

2.2. Reconnection Processes Observed in Solar Eruptions

There are two solar counterparts of the geomagnetic tail: One is the current sheet that extends from the top of flare loops and connects to the associated CME (e.g., see *Lin et al.* [2004]); and another one is embedded in the “helmet streamers”. Similarities of these two objects in morphology can be seen from both observations (e.g., see *Priest* [1982]) and numerical experiments (e.g., see *Birn et al.* [2003]). The current sheet configuration related to flares and CMEs cannot exist for long, and is created presumably by the disrupting magnetic field as a result of the loss of equilibrium in the system (e.g., see *Forbes and Isenberg* [1991]; *Forbes* [2000 and 2007]; and references therein). Such a scenario was suggested for the first time by *Carmichael* [1964], and was later developed into the well-known Kopp-Pneuman model [*Kopp and Pneuman* 1976], or more generally, the CSHKP model [e.g., see *Svestka and Cliver* 1992] (see Figure 2). It was further developed by *Martens and Kuin* [1989] and *Lin and Forbes* [2000] to the catastrophe model of the solar eruption in which the eruptive prominence evolves into the CME connecting to the associated flare below by a long current sheet (see Figure 3, and also *Lin et al.* [2003] for other models).

In this model, continuous mass motions and magnetic reconnection in the photosphere successively displace the footpoints of the coronal magnetic field, changes the shape of the field, converts the kinetic energy of mass motions into the magnetic energy and transports it into the corona. The low V_A and high β in the photosphere limits the rate of magnetic reconnection there such that no apparent heating and acceleration of plasma takes place (refer to Table 1). Instead the magnetic reconnection in the photosphere plays the role in transporting magnetic flux only. Here we note, again, the process of converting the kinetic energy from the low V_A and high β region (the photosphere) into magnetic energy stored in the high V_A and low β region (the corona). Eventually, when the stored energy in the corona exceeds the

threshold, the magnetic field loses the equilibrium and disrupts. Magnetic field lines are severely stretched to form an effectively open magnetic configuration including a neutral sheet separating magnetic fields of opposite polarity. Magnetic reconnection occurring inside the current sheet creates the growing flare loops in the corona and the separating flare loops on the solar disk (e.g., see *Forbes* [2000]; *Klimchuk* [2001]; *Priest and Forbes* [2002]; *Lin et al.* [2003]; *Birn et al.* [2003 and 2006]; *Forbes* [2007], and Figure 3 as well). When magnetic reconnection occurs in this current sheet, the high V_A and low β in the corona determines that the stored magnetic energy is released in a violent fashion.

Because the current sheet associated with flare and CME can only form and exist in the eruptive process, continuous reconnection analogous to that occurring at DNL in the Earth's tail ceases as the eruption ends. A typical eruptive process usually lasts tens of hours (e.g., see *Švestka and Cliver* [1992]), which may also be the lifetime of the corresponding continuous reconnection. The current sheet in the helmet streamer, on the other hand, can last much longer. The helmet streamer is the huge, long-lived, radially oriented structure that extends from the base of the corona out to several solar radii (e.g., see *Aschwanden* [2005], p. 9). The lower part of it contains closed magnetic field spanning over a magnetic neutral line on the solar surface, while the upper part turns into an open magnetic field joining the closed one in the region of the cusp-geometry from which the gas pressure starts to exceed the magnetic pressure outward. The long-lived property of the helmet streamer allows magnetic reconnection in the sheet to continue for a while analogous to that in the Earth's tail.

The helmet streamers will be discussed in the next section, and in this section we focus here on the CME/flare current sheet. Recent research indicates that the closed magnetic field does not necessarily become fully open as the Kopp-Pneuman-type eruption occurs. Instead, the magnetic structure is severely stretched and a current sheet forms [e.g., *Lin and Forbes* 2000; *Forbes and Lin* 2000]. With dissipation in the current sheet, the stretched magnetic field starts to reconnect, producing new closed field lines both below and above the current sheet [*Lin et al.* 2004], so the pre-existing closed magnetic field never becomes fully open (see Figure 3).

Related to the above theoretical results, a series of observations [*Ciaravella et al.* 2002; *Ko et al.* 2003; *Raymond et al.* 2003; *Sui and Holman* 2004; *Sui et al.* 2004; *Webb et al.* 2003; *Lin et al.* 2005; *Bemporad et al.* 2006] provided evidence for the formation and development of the long current sheets in major eruptions. Those of *Ko et al.* [2003], *Lin et al.* [2005], *Bemporad et al.* [2006], and *Lin et al.* [2007] further specified and analyzed the internal features of the long current sheets connecting solar flares to the associated CMEs. The most significant features are plasma blobs flowing away from the Sun along the sheets. Similar features flowing toward the Sun on the top of flare loops had been observed and identified with the reconnection outflow earlier [*Švestka et al.* 1998; *McKenzie and Hudson* 1999; *Sheeley and Wang* 2002; *Asai et al.* 2004; *Sheeley et al.* 2004], and numerical experiments for solar eruptions showed the blobs and flows moving in both directions [*Y. Fan* 2005, private communications; *Riley et al.* 2007].

The term “plasma blob” is not as well-known as plasmoid in either the solar physics or the geophysics communities since it was never used before *Ko et al.* [2003] who applied it to describing the flowing features along the reconnecting current sheet in an event producing a fast CME and an X-class flare (see their Figures 7 and 18). Subsequently, *Lin et al.* [2005] and *Riley et al.* [2007] observed similar features both in observations of another major event and in numerical experiments (see Figure 3 of *Lin et al.* [2005] and Figure 3 of *Riley et al.* [2007]). Following *Ko et al.* [2003],

they also utilized “plasma blobs” to describe these features. Comparison of the behavior and properties of plasma blobs observed in the solar eruption with those of plasmoids detected in the geomagnetic tail (see Figure 3 of *Hones* [1977], Figure 1.6 of *Birn and Priest* [2007], and Figure 1 of this work) suggests the identity of two objects appearing in different environments.

We also note that the term “flux rope” often appears in the literature of geophysics as well (e.g. *Slavin et al.* [1995]). The relevant structure is very similar to that of plasmoid flowing inside the geomagnetic tail, but *Sibeck et al.* [1984] also noticed several differences between the two. One of these important differences is the presence of an axial magnetic field inside the geo-flux-rope and the magnetic connection of the rope to the Earth (e.g., see discussions of *Moldwin and Hughes* [1991], and a recent numerical experiment by *Birn et al.* [2004]). This feature is quite like that of the flux rope in the solar environment, which includes a core field and is anchored to the Sun at its both ends (e.g., see *Lin et al.* [2004]).

Lin et al. [2007] and *Riley et al.* [2007] identified plasma blobs in the current sheet with the magnetic islands resulting from the tearing mode instability (turbulence). But such blob-like or island-like structures inside the reconnecting current sheets may also be ascribed to an alternative version of the energy conversion: the time-dependent Petschek-type reconnection [e.g., *Pudovkin and Semenov* 1985; *Priest and Forbes* 2000]. The theory of such a process was developed from the steady-state analysis of reconnection performed by *Petschek* [1964], and was then used to explain FTEs observed at the dayside magnetopause [see also *Rijnbeek et al.* 1989; *Semenov et al.* 1992; and references therein]. The slow mode shock has not yet been seen in the laboratory due to experimental difficulties [e.g., see *Hada and Kennel* 1985]. A possible approach to relating the observed plasma blobs to the reconnection outflow regions surrounded by the slow mode shock was recently discussed by *Lin et al.* [2007].

Compared with those detected in the magnetotail, the solar counterpart of the reconnection flows and the related features were not observed until *Švestka et al.* [1998] noticed a fan of spikelike ray structures above a group of flare loops observed by *Yohkoh*. Then, the apparent mass motion toward the Sun above the flare loop system in the long duration event of 1999 January 20 was reported by *McKenzie and Hudson* [1999]. Comparison with the standard model of two-ribbon flares [e.g., see *Forbes and Acton* 1996] suggests fitting of the observation to the theory. *McKenzie and Hudson* [1999] found that the late-phase downward motion was in the form of soft X-ray dark voids having speeds that vary from 100 km s^{-1} to 200 km s^{-1} , the temperature in this region reached up to $9.1 \times 10^6 \text{ K}$, and the density was a few times 10^9 cm^{-3} . These data indicate that the dark X-ray voids are the blobs, or magnetic islands in the reconnecting current sheet. Another 11 examples that showed similar Sun-ward flows during the long-duration events observed by *Yohkoh* SXT were also reported by *McKenzie* [2000]. The speeds of those flows ranged from 50 km s^{-1} to 500 km s^{-1} , and all the events were associated with CMEs.

Subsequently, a series of plasma downflows above the post-flare loops were successively observed. *Sheeley and Wang* [2002] reported the coronal downflows observed with LASCO 2–6 R_\odot from the heliocenter. The maximum velocities of individual downflows varied from 50 km s^{-1} to 100 km s^{-1} . The well-known TRACE event that occurred on April 21, 2002 gave rise to an X1.2 class flare and a very fast CME ($\geq 2500 \text{ km s}^{-1}$). It was also well observed by the instruments on SOHO, such as LASCO, SUMER, EIT, and UVCS [*Innes et al.* 2003; *Raymond et al.* 2003; *Sheeley et al.* 2004]. The downward flow features were observed at the early stage of the eruption, and both the speed and

temperature of the plasma flow were fairly high (up to 1000 km s⁻¹ and a few times 10⁷ K, respectively). *Sheeley et al.* [2004] employed a technique developed to study motions in the outer corona [see *Sheeley et al.* 1999] to track the plasma downflows displayed by this event (Figure 4). What is nice about their technique is that it helps manifest in a very clear way several important features related to magnetic reconnection. These features include the fast reconnection outflow (100 – 600 km s⁻¹) towards the flare loops and the significant deceleration (~ 1500 m s⁻²) of the flows at the top of the flare loop system, which is highly suggestive of the reconnection outflow encountering the closed field line region in the magnetotail context (refer to those nightside closed field lines in Figure 1 and those below the current sheet in Figure 2b).

Asai et al. [2004] presented a detailed study of downward motions above flare loops observed in the July 23, 2002 event. This event produced an X4.8 flare and an energetic CME (~ 2600 km s⁻¹), and was well observed by TRACE, RHESSI, NoRH, UVCS, and LASCO [*Emslie et al.* 2003; *Raymond et al.* 2003]. During this event, the downflows above the post-flare loops were seen not only in the decay phase but also in the impulsive and main phases, and showed clear correlation to the non-thermal emissions in microwaves and HXRs. Magnetic reconnection was thought to account for these characteristics. Most recently, a limb flare was observed by SOHO/SUMER, TRACE, and RHESSI, and the sunward reconnection outflows consisting of hot plasma along the flare loops was reported by *Wang et al.* [2007].

Because of the relatively small scale and the low emission measure of the current sheets in the solar eruption, the magnetic reconnection outflow moving away from the Sun was not noticed until a major eruptive process was observed by *Ko et al.* [2003] that developed a typical CME–current sheet–flare loop system. A series of plasma blobs moved along the sheet continuously (Figure 5), and five of them were well characterized, allowing us to further study important properties of the current sheet [*Lin et al.* 2007]. Later, another event that developed similar morphological features in the disrupting magnetic field was observed (Figure 6), *Lin et al.* [2005] identified five well observed blobs, and *Riley et al.* [2007] recognized four.

In the numerical experiments of *Forbes and Malherbe* [1991], *Y. Fan* [2005, private communication], and *Riley et al.* [2007], the repeated formation of a set of blobs that move both toward and away from the Sun occurred. Although these numerical experiments were not performed to model any specific event, there is good general agreement in the formation of the current sheets and the formation and propagation of the blobs flowing along the sheet. *Forbes and Malherbe* [1991] and *Riley et al.* [2007] pointed out that the formation and evolution of the blob in the sheets are strongly suggestive of the tearing mode instability [e.g., *Furth et al.* 1963] that plays an important role in magnetic field diffusion and governing the scale of the sheet [*Strauss* 1988; *Drake et al.* 2006]. More investigations indicate that the turbulent diffusion caused by the tearing mode could be much faster or more efficient than that caused by the classical and anomalous resistivities [*Strauss* 1988; *Bhattacharjee and Yuan* 1995].

Alternatively, the formation and propagation of plasma blobs may be explained within the framework of unsteady Petschek-type reconnection. This approach has been employed in the modeling of reconnection in the terrestrial context [e.g., *Biernat et al.* 1987; *Seon et al.* 1996; *Eriksson et al.* 2004]. Because at present *in situ* measurements are not available to document solar activities, we are not able to confirm whether slow shocks would develop during the eruption. But the heating and evaporation of the chromosphere in the flare process may constitute the indirect evidence of the formation and propagation of the slow mode shocks [e.g.,

see *Forbes and Acton* 1996], and our knowledge about the reconnection process in the magnetotail also suggests the likelihood of the slow mode shocks forming in CME/flare current sheets.

The reconnection outflow along the CME/flare current sheet discussed above also shows similar flowing features to those occurring in the geomagnetic tail (e.g., see *Slavin et al.* [2003 and 2005]). These features include both sunward and anti-sunward flows. The sunward flow was usually observed to decelerate apparently near the top of the flare loop system [*Sheeley et al.* 2004; *Asai et al.* 2004] as a result of deflecting and ceasing by the closed flare loops (e.g., see also *Reeves et al.* [2008]). Observations indicate as well that the two reconnection outflows separate at one of multiple X-points (the joint points of every two adjacent plasma blobs or plasmoids) in the sheet (cf. plasma flows observed by *McKenzie and Hudson* [1999], *Sheeley et al.* [2004], and *Asai et al.* [2004] with those observed by *Ko et al.* [2003] and *Lin et al.* [2005], as well as the numerical experiment by *Riley et al.* [2007]). This special X-point becomes dominant in the eruption and usually does not move with the reconnection flow. Similar to the case in the magnetotail, we do not well understand for the time being the physical mechanism that determines the location of this dominant X-point. But the above observations and numerical experiments suggest that it be somewhere between 0.5 and 1.0 R_{\odot} from the surface of the Sun, and that it is probably governed by the nearby plasma and magnetic environment.

2.3. Mass Flows of Various Scales in the Solar Wind

Mass flows of various length scales occur ubiquitously in the solar wind. Among these flows, the largest feature is the ICME, which is the most important product of solar activity in the interplanetary medium, and is produced by a rapid release of magnetic energy in the solar eruptive process [*Lin et al.* 2004 and references therein]. An important subset of these is the magnetic clouds [*Burlaga et al.* 1981; *Klein and Burlaga* 1982], which are observed at 1 AU as mesoscale (fraction of an AU) configurations characterized by a magnetic field of above-average strength executing a large and smooth rotation in a plasma of low proton temperature and β . Their magnetic field structure has been modeled as cylindrically-symmetric, constant- α force-free magnetic flux ropes of circular cross-section, a solution of which was given by *Lundquist* [1950], and has been applied in an interplanetary context by *Burlaga* [1988], *Lepping et al.* [1991], and many others. The feet of magnetic clouds may still be anchored at the Sun, and examples of such events were reported by *Farrugia et al.* [1993b and 1993c] and *Shodhun et al.* [2000].

Smaller scale flux ropes in the solar wind during quiet times were also reported by *Moldwin et al.* [2000]. Their average diameter is of order a few percent that of magnetic clouds, but in all other aspects they are similar to clouds. As generating cause, we suggest reconnection in the heliospheric current sheet (as opposed to the corona for magnetic clouds). Below we shall discuss small-scale reconnection in the heliospheric current sheet related to the papers of *Gosling et al.* [2007 and references therein] and co-workers.

There is a great deal of evidence from both UVCS/SOHO observations and *in situ* measurements that magnetic reconnection continues to occur as the solar wind accelerates and expands throughout the heliosphere [*Kohl et al.* 2006; *Gosling et al.* 2007]. The island-like features are frequently observed in the slow solar wind, which is believed to originate (at least in part) from bright “helmet streamers” that have been seen in white-light coronagraph images for decades. But it is uncertain how the plasma expands into a roughly time-steady flow since many of these streamers appear to have a closed magnetic field. Outflow speeds measured by the UVCS instrument on SOHO appear to be consistent with the *in situ* slow wind along the open-field edges

(or “legs”) of large streamers [Strachan *et al.* 2002]. The closed-field “core” regions of streamers, on the other hand, exhibit negligible outflow speeds and anomalously low ion abundances [e.g., Raymond *et al.* 1997]. These observations provide strong evidence for the idea that the majority of the slow wind originates along the open-field edges of streamers.

However, evidence also exists for a time-variable plasmoid-like component of the slow wind in streamers. The increased photon sensitivity of the LASCO/SOHO white-light coronagraph over earlier instruments revealed an almost continual release of low-contrast density inhomogeneities, or “blobs,” from the cusps of streamers [Sheeley *et al.* 1997]. These features appear to accelerate to velocities of order 300 to 400 km s⁻¹ by the time they reach $\sim 30 R_{\odot}$, the outer limit of LASCO’s field of view. Because of their low contrast, though (i.e., they represent only about 10% changes from the time-averaged streamer), the blobs probably do not comprise a large fraction of the mass flux of the slow solar wind.

Wang *et al.* [2000] reviewed three general scenarios for the production of these blobs: (1) “streamer evaporation” as the loop-tops (with plasma $\beta \approx 1$) are heated to the point where magnetic tension is overcome by high gas pressure; (2) plasmoid formation as the distended streamer cusp pinches off the gas above an X-type neutral point; and (3) reconnection between one leg of the streamer and an adjacent open field line, transferring some of the trapped plasma from the former to the latter and allowing it to escape [see Figure 8 of Wang *et al.* 2000]. They concluded that all three mechanisms might be acting simultaneously [see also Wu *et al.* 2000; Fisk and Schwadron 2001; Lapenta and Knoll 2005]. Einaudi *et al.* [1999; 2001] performed hydrodynamical simulations of the narrow shear layer above the streamer cusp and found that magnetic islands can form naturally as the nonlinear development of a tearing-mode instability.

There may be some similarity between these scenarios and older models of diamagnetic acceleration of the solar wind via buoyant plasmoids that may fill some fraction of the corona [e.g., Schlüter 1957; Pneuman 1986; Mullan 1990]. The additional momentum deposited by this process is given approximately by an effective buoyancy-driven pressure gradient

$$a_d = -\frac{3}{2} f_d w_d^2 \frac{\partial}{\partial r} \left(\ln \frac{B_0^2}{8\pi} \right), \quad (1)$$

where f_d is the ratio of mass flux in the plasmoids to the total wind mass flux and w_d is the most-probable speed in the plasmoids [see also Pneuman 1983; Yang and Schunk 1989; Tamano 1991]. Plasmoid inhomogeneities may arise from reconnection events [e.g., Yokoyama and Shibata 1996] and expand to fill a large fraction of the volume of coronal holes [see also Feldman *et al.* 1997].

At some point in the outer solar atmosphere, MHD turbulence develops from the underlying waves and/or field-line motions (e.g., see Coleman [1968]; Goldstein *et al.* [1995]; Tu and Marsch [1995]). The energy flux in the turbulent cascade has been proposed as a natural means of heating the corona and accelerating the solar wind [Hollweg 1986; Matthaeus *et al.* 1999; Cranmer *et al.* 2007]. Interestingly, on the smallest spatial scales, MHD turbulence has been shown to develop into a collection of narrow current sheets undergoing oblique magnetic reconnection (i.e., with the strong “guide field” remaining relatively unchanged). There is increasing evidence for the presence of such small-scale reconnection regions in both the slow solar wind [Gosling *et al.* 2005, 2006] and the fast solar wind [Gosling *et al.* 2007], both of which are strongly turbulent. These *in situ* measurements generally pinpoint regions of fast jetlike “exhaust” bounded by pairs of back-to-back rotational discontinuities in solar wind streams having low plasma beta ($\beta < 1$). Reconnection in these regions has been suggested as a possibly

important channel for maintaining the extended heating of the solar wind (e.g., Leamon *et al.* [2000]).

Small-scale current sheets and plasmoids arise spontaneously in numerical simulations of MHD turbulence. These simulations are generally not seeded with any kind of forced reconnection. The coherent structures arise from the natural stochastic evolution of the fields (e.g., see Kinney *et al.* [1995]; Mininni *et al.* [2006]). Dmitruk *et al.* [2004] and Dmitruk and Matthaeus [2006] performed test-particle simulations in a turbulent plasma that contains the kinds of reconnection regions described above. They found that protons can become perpendicularly accelerated around the guide field because of coherent forcing from the perturbed fields associated with the current sheets. Also, Markovskii *et al.* [2006] found that the intensified shear motions across these current sheets can lead to an unstable growth of waves near harmonics of the ion-cyclotron frequency. These ideas may be important ingredients in the production of preferential heating and acceleration of heavy ions in the extended solar corona, as observed by UVCS/SOHO (e.g., see Kohl *et al.* [1997 and 2006]).

3. Mechanisms for Producing Plasmoids (Plasma Blobs)

Small scale structures turn out to be ubiquitous in reconnecting current sheets in various circumstances. Their existence is essential for improving the efficiency of energy conversion through magnetic reconnection, and thus for enhancing the rate of reconnection. In the framework of plasma physics, these structures are ascribed to plasma instabilities and the corresponding modes of turbulence; and in the framework of MHD, on the other hand, they could be the reconnection outflow regions surrounded with the slow mode shocks. Here, we discuss these two scenarios and their implications for observations. It is difficult to distinguish between them on the observational evidence we have at present.

3.1. Current Sheets Undergoing Tearing

Traditional Sweet-Parker reconnection [Sweet 1958a and 1958b; Parker 1957 and 1963] is too slow to account for the rate of energy conversion occurring in either the geomagnetic substorm or the solar eruption. The low rate of energy conversion results from the large scale of the diffusion region. Reducing such a scale helps the energy conversion become more efficient. Minimizing the diffusion region scale in a large (long) current sheet could be well accomplished by the plasma turbulence invoked by various instabilities (e.g., Furth *et al.* [1963]; Ambrosiano *et al.* [1988]; Lazarian and Vishniac [1999]; Priest and Forbes [2000]; Drake *et al.* [2006]). In this case, the scale of the diffusion region is roughly that of the turbulence eddies, or magnetic islands, which is much smaller than the global length scale of the system, and yields higher reconnection rate [Strauss 1988; Bhattarjee and Yuan 1995]. The reconnecting current sheet in such a framework is an assembly of many modes of turbulence or the filamental current sheets and reconnection exhausts, which is the typical scenario of turbulence reconnection.

Among these instabilities, the tearing mode is one of the most extensively studied. It is a long-wavelength, resistive instability. It was investigated for the first time by Furth *et al.* [1963] in the framework of resistive instability modes established by Dungey [1958], which showed that at an X-type neutral point configuration in the magnetized plasma, finite conductivity (or resistivity) can give rise to an unstable growing current concentration. By this mechanism, a sheet pinch, or a current sheet, can tear along current-flow

lines, forming a chain of filaments, or magnetic islands in projection (Figure 7). Here k is the wave number of the turbulence caused by the instability and $l = d/2$ is the half thickness of the sheet.

Properties of the magnetized plasma require that the growth rate of the modes considered be slow compared to the hydromagnetic rate, but fast compared to the resistive diffusion rate. In the case of the tearing mode, this relates k to l by [Furth *et al.* 1963]

$$S^{-1/4} < kl < 1, \quad (2)$$

where $S = \tau_d/\tau_A$ is the Lundquist number of the current sheet, $\tau_A = l/V_A$ and $\tau_d = l^2/\eta$ are the times at which the Alfvén wave and the resistive diffusion traverse the sheet, respectively. Here, V_A is the local Alfvén speed near the current sheet, and η is the magnetic diffusivity of the sheet. The turbulence caused by the instability broadens the current sheet significantly so that $S \gg 1$ usually holds in most circumstances. From the definition of S , we have $S = lV_A/\eta$.

According to the standard theory of magnetic reconnection, the magnetic field is continuously being dissipated through the current sheet at the same rate as magnetic flux is brought into the sheet, which leads to [e.g., see Priest and Forbes 2000, p. 120]:

$$v_i = \frac{\eta}{l}, \quad \text{with } \eta = \frac{\eta_e}{\mu_0}, \quad (3)$$

where v_i is the reconnection inflow speed in units of m s^{-1} , η is in units of $\text{m}^2 \text{s}^{-1}$, η_e is the electric resistivity in ohm m, and $\mu_0 = 4\pi \times 10^{-7} \text{ H m}^{-1}$. Then we end up with

$$S = V_A/v_i = M_A^{-1}, \quad (4)$$

where M_A is the Alfvén Mach number, the rate of magnetic reconnection measured as v_i/V_A , which is also known as the relative reconnection rate compared to the absolute reconnection rate that is measured as the reconnecting electric field in the current sheet (see discussions by Lin and Forbes [2000] and Priest and Forbes [2000], on this issue). Equation (4) relates S directly to M_A , a quantity that can be deduced from observations.

After going through simple algebra, we find from $kl > S^{-1/4}$ of (2):

$$l_{min} = k^{-1}S^{-1/4} = M_A^{1/4} \frac{\lambda}{2\pi}, \quad (5)$$

where λ is the wavelength of the turbulence (see Figure 7), and is identified with the distance of two successive plasma blobs flowing along the current sheet [see Ko *et al.* 2003; Lin *et al.* 2005]. Therefore, equation (5) relates l_{min} to M_A and λ in a simple and straightforward fashion. Usually, M_A in reality varies from 10^{-3} to 10^{-1} for solar events and laboratory plasma [e.g., Furth *et al.* 1963; Priest and Forbes 2000; Yokoyama *et al.* 2001; Ko *et al.* 2003; Lin *et al.* 2005], and from 10^{-2} to 10^{-1} for the reconnection processes in both the magnetopause [Vaivads *et al.* 2004; Rentina *et al.* 2007; references therein] and the magnetotail [Xiao *et al.* 2007; references therein]. Thus in these disparate contexts, M_A has approximately the same range of variation.

These values of M_A indicate that $S \gg 1$ usually holds for both solar and geomagnetic cases, but $S^{1/4} \gg 1$ does not. Instead, $S^{1/4} > 1$ holds marginally for most of these values of M_A . Hence, by inequalities in (2), quantity kl could possess a finite lower limit. Direct observations of the CME/flare current sheets indicate that the sheet thickness varies from 10^4 to 10^5 km [Lin *et al.* 2007], and *in situ* measurements of the magnetopause and the magnetotail estimate a thickness ranging from 200 to 500 km [Vaivads *et al.* 2004; Xiao *et al.* 2007].

Because of the size of the sheet thickness and the energy of the electrons there contained, collisionless effects (such as

Spitzer resistivity) cannot play a role in the dynamics of the current sheet. Instead, the relevant processes are collisionless with macroscopic effects that transform magnetic energy into plasma kinetic and thermal energy, and could account for various timescales of the phenomena during auroral events in the auroral regions and in the magnetotail [Coppi 1965]. However, subsequent investigations on the tearing mode in the magnetotail [Pritchett and Coroniti 1990; Pritchett *et al.* 1991] revealed that the ion tearing mode is unlikely to develop spontaneously in the closed field line region of the near-Earth plasma sheet, but external influences and time-dependent effects (with the attempt to establish large-scale convection flow) might be able to trigger the tearing mode instability and lead to rapid reconnection.

Collisionless effects become dominant when the resistive scale size is smaller than the ion skin depth, $\sqrt{m_i c^2/(4\pi n_i e^2)}$, where m_i is the ion mass, n_i is the number density, e is the charge. In this case a separation of ions and electrons results. The ions decouple from the magnetic field in the ion diffusion region. Eventually, inside the smaller electron diffusion region, the electrons, too, become demagnetized [Vasyliunas 1974]. The separation of ions and electrons in the ion diffusion region produces a system of currents (Hall currents) which induce a quadrupolar Hall magnetic field pattern [Sonnerup 1979]. This outlines a scenario of collisionless tearing mode turbulence and its observational consequences, and the formation of Hall magnetic and electric field structure in the vicinity of the diffusion region is a key feature of collisionless magnetic reconnection.

Investigations of collisionless reconnection by means of particle simulations were reported in the context of the geospace environmental modeling reconnection challenge by Birn *et al.* [2001]. Another example of studying collisionless reconnection via particle-in-cell simulations was conducted recently by Shay *et al.* [2007]. They demonstrated that reconnection remains fast in very large systems. The electron dissipation region develops a distinct two-scale structure along the outflow direction. Consistent with fast reconnection, the length of the electron current layer stabilizes and decreases with decreasing electron mass, approaching the ion inertial length for a proton-electron plasma. They found that the electrons form a super-Alfvénic outflow jet that remains decoupled from the magnetic field and extends large distances downstream from the X-line.

In the magnetotail context, a number of spacecraft observations have been reported where the quadrupolar Hall magnetic fields were detected. When a spacecraft traverses the magnetotail reconnection region from one side of the X-line to the other, it could confirm the presence of the Hall quadrupolar fields, and by implication the importance of collisionless effects in reconnection, if it observed a reversal of the out-of-plane (i.e. parallel to the X-line) magnetic field component [Shay *et al.* 2001]. The Hall quadrupolar magnetic fields have been observed by the Geotail spacecraft in the near-Earth region [Naqai *et al.* 2001] outside the diffusion region. *In situ* detection of signatures of Hall currents were presented by Øieroset *et al.* [2001], who analyzed data returned by the Wind spacecraft as it traversed the near-Earth ($\sim 60 R_E$) geomagnetic tail going from the earthward to tailward side of the X-line.

In the solar context, considering plasma properties of the coronal environment, magnetic reconnection occurring in the corona is collisionless as well. It has now been suggested that the collisionless aspects of reconnection are important to regulate the rate of coronal heating (e.g., see recent works by Cassak *et al.* [2006 and 2008]; Uzdensky [2007]), in addition to that releasing the magnetic energy in the CME/flare current sheet as shown in Figure 3.

Recent multi-point Cluster observations were conducted by *Eastwood et al.* [2007]. They observed a reconnection event in the near-Earth magnetotail where the diffusion region was nested by the Cluster spacecraft. They found that, close to the diffusion region, the magnetic field displays a symmetric quadrupole structure, the Hall electric field is strong (up to $\sim 40 \text{ mV m}^{-1}$) on the earthward side of the diffusion region, but substantially weaker on the tailward side. In conjunction with these observations, a small-scale magnetic flux rope was observed. It was located in the plasma flow near the reconnection site and may be the secondary islands appearing in numerical experiments. A very strong Hall electric field (up to $\sim 100 \text{ mV m}^{-1}$) inside the magnetic island was detected.

3.2. Other Types of Multiple X-Line Reconnection

In addition to the tearing mode instability and the consequent turbulence, other possibilities exist responsible for the magnetic island formation in the reconnecting current sheets. Among these possibilities is the Petschek reconnection, which was first investigated by *Petschek* [1964] for the steady-state case. Considering the time-dependent behaviors of the process in both solar flares and substorms in the magnetosphere, Petschek's original model was developed to the time-dependent version (e.g., see *Pudovkin and Semenov* [1985]; *Biernat et al.* [1987]; *Priest and Forbes* [2000], pp. 222–229).

In this framework, the classical Ohmic diffusion is confined to a small region, and disturbance caused by the diffusion generates the slow mode shocks propagating rapidly into the surrounding plasma medium, and transmitting the diffusion-associated disturbances into the system at large [e.g., see *Biernat et al.* 1987]. There is a self-adjustment between the large scale field and plasma flow distribution and the reconnection rate, so the evolutionary behavior of the hydromagnetic configuration is ultimately governed both by the globally imposed boundary conditions and the local processes occurring inside the diffusion region, which is described by the time-dependent Alfvén Mach number $M_A(t)$.

As examples, we study the response of the medium to the following two time profiles of M_A :

$$M_A(t) = \begin{cases} \frac{5}{8}t^2(t-1)^2 & \text{for } 0 < t < 1 \\ 0 & \text{otherwise,} \end{cases} \quad (6)$$

and

$$M_A(t) = \frac{1}{20}[1 - \cos(2\pi t)], \quad (7)$$

where t is in units of τ_A . Time profiles of these two M_A s are plot in Figures 8a and 8b, respectively. Magnetic reconnection described by (6) commences at $t = 0$, reaches its maximum 0.1 at $t = 0.5$ and ceases at $t = 1$.

In the case of single pulse reconnection, the response of the medium is displayed in Figure 9a. The disturbance commences at the origin (namely the diffusion region marked with asterisk) as $t = 0$, and propagates at the local Alfvén speed, which is larger than the slow magnetoacoustic speed, so the slow mode shock forms in front of the propagating disturbance ($t = 0.5$). Collectively, these slow shocks establish an outflow region for plasma and magnetic field streaming along the current sheet. Upstream of the shock, the medium is unperturbed due to the finite propagating speed of the disturbance. With reconnection ceasing after $t = 1.0$, no further perturbation is produced from the diffusion region, the outflow region and the slow shocks are detached from the original diffusion region, the current sheet is re-established in the wake of the outflow region ($t \geq 1.0$), and the reconnection inflow is prevented but the outflow regions

keeps propagating and expanding. (Note: Detailed formulations for magnetic configurations in this figure and in Figure 9b below can be found in *Biernat et al.* [1987] and /or *Priest and Forbes* [2000, pp. 222–239]. We do not duplicate them here.)

Magnetic reconnection described by (7) produces a different evolution in the system. It commences at $t = 0$, but does not cease. So a series of reconnection outflow regions associated with slow shocks are continuously formed and move away from the diffusion region (Figure 9b). This corresponds to a bursty reconnection scenario in which plasma blobs or plasmoids are observed to develop successively (see also *Riley et al.* [2007] for examples of numerical experiments). It represents some important features of the multiple X-line reconnection process as well. We note that we use the single pulse reconnection here as an example to demonstrate how the impact of the magnetic diffusion occurring in a local region could cause disturbance and energy conversion in the medium at large. But it may not be the fashion in which magnetic reconnection takes place in reality. Instead, bursty reconnection is more likely to occur in both solar and magnetospheric environments.

The most significant consequence of introducing the slow mode shocks attached to the diffusion region is the tremendous enhancement of the energy conversion rate, or the rate of magnetic reconnection since the slow mode shock is also known as a switch-off shock through which the downstream tangential magnetic field is almost switched off, and the corresponding magnetic energy is converted into heating and kinetic energy of the reconnected plasma [*Priest* 1982]. The density, the pressure, and the temperature of the reconnected plasma in the outflow region increase by a factor of

$$r_n = \frac{\gamma(\beta+1)}{\gamma(\beta+1)-1}, \quad r_p = \frac{\beta+1}{\beta}, \quad \text{and} \\ r_T = \frac{\beta+1}{\beta} \frac{\gamma(\beta+1)-1}{\gamma(\beta+1)} \quad (8)$$

respectively, with γ being the ratio of specific heats and β being the plasma beta (e.g., see *Pudovkin and Semenov* [1985]). Usually, $\gamma = 5/3$, so equations in (8) implies significant heating when reconnection occurs in the force-free ($\beta \ll 1$) environment like the solar corona and the magnetotail lobes, very weak heating in the large β environment like the photosphere and the dayside magnetopause (refer to Table 1).

In the solar corona, the consequences of the bursty reconnection are identified in several eruptive events that have been well studied (see Figures 4, 5, and 6), and the slow mode shock may also account for observations of high temperature emissions [*Innes et al.* 2001; *Ciaravella et al.* 2002; *Ko et al.* 2003; *Raymond et al.* 2003]. In the Earth's magnetotail, such a reconnection mode has been widely held to be a mechanism by which plasmoids/magnetic flux ropes are produced. This view is grounded on analytical modeling (e.g. *Schindler* [1974]), and extensive numerical simulations [*Hesse and Birn* 1991; *Hesse et al.* 1996; *Hesse and Kivelson* 1998; and references therein]. There is also the work of *Fu and Lee* [1985] on multiple X-line formation that will be discussed shortly. The events associated with the slow mode shocks have been reported as well (e.g., see *Seon et al.* [1996]; *Eriksson et al.* [2004]; and also *Priest and Forbes* [2000], pp. 343–344 for a brief overview). A reconnection layer in the solar wind where slow mode shocks were tentatively identified was given by *Farrugia et al.* [2001].

Scaling laws associated with the formation of the slow mode shocks connect the current sheet thickness to the extension of the slow mode shocks, and can be deduced from the shape or structure of the slow mode shocks. From equations (11) and (17c) of *Biernat et al.* [1987], or equivalently

equation (7.47) of *Priest and Forbes* [2000], we find the average sheet thickness \bar{l} can be related to the average extension of the shock $\bar{\lambda}$ via the average rate of magnetic reconnection \bar{M}_A

$$\bar{l} \approx r_n^{-1} \bar{M}_A \bar{\lambda}, \quad (9)$$

in the Petschek reconnection process. Here \bar{M}_A and $\bar{\lambda}$ are obtained by taking averages of $M_A(t)$ over the time domain and of the shock extension over the space domain in x -direction (see Figure 9), respectively, with keeping the fact in mind that the medium upstream of the shock remains unperturbed before the shock arrives. Forms of those equations used to deduce 9 are simple and the algebra performed are straightforward, so we do not duplicate them here and skip the algebra. Similar to (5), equation (9) relates several important parameters for magnetic reconnection to one another, and these parameters are all observables. Such relations provide us opportunities to look into some crucial properties of energy conversion through magnetic reconnection in either the magnetosphere or the solar corona, and may help tell what type of reconnection is occurring or has occurred by comparing theories and observations.

We notice the similarity of equation (9) to (5) in that l is related to λ linearly although these two equations are deduced in different frameworks. Such as similarity is quite likely to suggest a kind of equivalence in physics of the two frameworks in which the reconnection process is studied. This is probably because both turbulent eddies and shocks act as diffusion structures which play an important role in converting energy from one form into another. If we enlarge the fine structures of the turbulent current sheet, we may find that each magnetic island-neutral point-magnetic island structure inside the turbulent current sheet in Figure 7 can be seen as a Petschek-type reconnection morphology displayed in Figure 9 in small scale, and a turbulent sheet should be full of numerous such small scale structures [see *Drake et al.* 2006; *Rentinò et al.* 2007].

In fact, both the turbulence and the Petschek versions of reconnection were used to explain the same results of a numerical experiment. In their original work on the numerical simulation of magnetic reconnection occurring in the current sheet extending from the top of the flare loop system, *Forbes and Malherbe* [1991] identified the plasma blobs appearing in the sheet with the magnetic islands caused by the tearing mode. But *Priest and Forbes* [2000, pp. 391–393] explained these blobs within the framework of the Petschek-type reconnection. That alternative versions of reconnection were used to account for the same result of numerical experiment should somehow imply the viability of the two approaches to investigating and describing the reconnection process. Furthermore, this might suggest that both versions of reconnection operate together in the eruptive event in reality. At present this issue requires further investigations.

In addition, multiple X-line reconnection may occur in a different fashion. Numerical investigations of the plasma dynamics of a long magnetotail ($\sim 200R_E$) indicated that the formation of X-line and plasmoids occurs intermittently and repeatedly every 2–4 hours [*Lee et al.* 1985], and reconnection in the magnetotail during substorms and storms is basically a driven process. These results are consistent with some observations made in the magnetotail. The force driving reconnection is governed by the environment and manifests time-dependent features, which may account for the time profile of M_A discussed above. The formation and evolution of a three-dimensional plasmoid in the geomagnetic tail was numerically studied by *Hesse and Birn* [1991]. The configuration investigated includes the transition from a closed field line region to an open far-tail region with a distant X-line. They found that the formation and growth of a plasmoid body through reconnection occurs in the near-Earth region, and helical plasmoid field lines are produced but remain connected to the Earth.

Besides the phenomena in the magnetotail, the multiple X-line reconnection may also result in FTE's observed by ISEE satellites at the dayside magnetopause [*Lee and Fu* 1985]. Existence of the skew components of the reconnected field lines allows the formation of the flux rope consisting of the helical field lines. In this model the magnetic island is not isolated but is part of an interconnected chain of two-dimensional X-points and O-points. Further studies showed that the occurrence of the multiple X-line reconnection is governed by the current sheet scales [*Fu and Lee* 1985]. This process is expected to happen when the sheet length is large compared to its thickness and the resistivity is low. *Lee and Fu* [1986] found as the ratio λ/l exceeds a critical value between 10 and 20, multiple X-lines are observed to appear in the current sheet.

Lee [1990] noted that with the formation of a long current sheet in the magnetopause, the non-uniformity of the solar wind pressure and the stress of interplanetary magnetic flux exerted on the magnetopause surface may also cause variations in the current density and, consequently, reconnection to occur at several locations. Associated with the successive appearance of multiple X-lines and plasmoids is bursty reconnection rate or electric field [*Lee et al.* 1990], which resembles that shown in Figure 8b. As we already mentioned before, features of multiple X-line reconnection have also been recognized in both magnetotail substorms [*Slavin et al.* 2003 and 2005] and solar eruptive events [*Ko et al.* 2003; *Lin et al.* 2005], as well as in the numerical experiments for solar eruptions [*Riley et al.* 2007].

Before ending this section, we believe it is also worth mentioning the work by *Lazarian and Vishniac* [1999] who studied the role of the stochastic features in the current sheet through a different approach. In this version of energy conversion, magnetic field dissipation starts with Ohmic diffusion. Then, stochastic components of the magnetic field are produced in the initial stage. With the occurrence of stochastic components, there is small-scale “wandering” in the field lines. This allows magnetic reconnection to take place among adjacent wandering field lines (see Figure 2 of *Lazarian and Vishniac* [1999]), yielding multiple reconnection sites within the sheet. The presence of multiple reconnection sites results in a minimum rate of reconnection, $M_A = R_L^{-3/16}$, where R_L is the magnetic Reynolds number in the whole system involved in the energy conversion. In the solar coronal R_L ranges from 10^8 to 10^{12} , which brings the minimum of M_A to 5.6×10^{-3} that is within the range of the observed values that we have known so far.

4. Discussion

In this work we have engaged in a comparative study of the reconnection process in the solar and terrestrial contexts. Properties of the magnetized plasma determines that the rate of reconnection in both environments is controlled by the local Alfvén speed. This further yields that the reconnection process in the low V_A and high β region transports magnetic flux and energy to the region of high V_A and low β gradually, and that reconnection in the high V_A and low β region releases the stored magnetic energy violently. This may explain why the consequences occurring in the photosphere and in the dayside magnetopause (low V_A and high β) are much less significant than those occurring in the corona (flares and CMEs) and in the magnetotail (substorms) (high V_A and low β).

Of course, because of the huge difference in scale length and magnetic field strength, the absolute amount of energy conversion and the absolute rate of reconnection (usually measured by the strength of reconnection electric field

along the X-line) in the solar and terrestrial contexts could greatly differ from one another. For example, a typical solar eruption involves energy release of up to 10^{32} ergs (e.g., see *Priest* [1982]) and the absolute reconnection rate typical varies from 1 V/cm to 10 V/cm (e.g., see *Poletto and Kopp* [1986] and *Qiu et al.* [2004]), and a typical substorm releases energy of only $10^{21} \sim 10^{22}$ ergs [*Baker et al.* 1997] and the absolute reconnection rate of $1 \sim 10$ mV/m (e.g., see *Blanchard et al.* [1997] and *Vaivads et al.* [2006]).

On the other hand, the rate of reconnection is also often measured by the Alfvén Mach number M_A , which is the reconnection inflow speed v_i compared to the local Alfvén speed V_A near the reconnection region. So M_A is known as the relative reconnection rate as well (e.g., see discussions of *Lin and Forbes* [2000] and *Priest and Forbes* [2000]). In this sense, M_A is within the same order of magnitudes between 0.01 and 0.1 for the reconnection processes in both solar and magnetospheric environments (cf. *Ko et al.* [2003], *Lin et al.* [2005] and *Vaivads et al.* [2006]) although the absolute rates of reconnection in the two environments are vastly different. This result should help us study and well understand the similar energy conversion processes taking place on other objects in the universe.

Another emphasis related to reconnection has been the formation of plasmoids/plasma blobs in both environments. The magnetic reconnection process manifests almost the same features in various different magnetized plasma environments, including the solar corona and the magnetosphere. Usually flows are observed in two opposite directions along the sheet in both the magnetotail and the CME/flare sheet, and only the antisunward flow is observed in the helmet streamer. This is probably because the reconnection in the helmet streamer is weaker and the sunward reconnection outflow is easily stopped by the closed loops below. Plasmoids or plasma blobs flowing along the reconnecting current sheet are the ubiquitous features observed in these environments although mechanisms for the formation the current sheet vary from case to case.

These plasmoids are usually ascribed to multiple X-line reconnection as a result of the tearing mode instability developing in a long thin current sheet (e.g., see *Furth et al.* [1963] and *Priest* [1985] for the review; and *Drake et al.* [2006] and *Loureiro et al.* [2007] for the most recent works on this topic). Reconnection occurs at each of these X-lines, but one of them eventually develops to become the dominant one at which the fastest reconnection takes place, and its high speed flow expels both plasmoids and other X-lines to move in two opposite directions. The mechanism determining the location of this dominant X-line is an open question, but it should depend on the parameters of the plasma and magnetic field around.

An alternative process that may account for the plasmoid feature is time-dependent Petschek-type reconnection extensively studied by *Semenov* and his co-authors. In this framework, diffusion initially commences somewhere in a pre-existing current sheet where a finite electrical resistivity appears. The impact caused by the diffusion is not confined to the diffusion region but propagates as a disturbance at the local Alfvén speed to the medium at large. Determined by the time profile of the diffusion, the disturbance propagates along the current sheet with two pairs of the slow mode shocks surrounding the reconnected plasma and magnetic field in the outflow region. Departing from the diffusion region, the two pairs of the slow shock and the associated plasma flows propagate in opposite direction. In this case, multiple X-lines and blobs may appear alternatively along the sheet, but the dissipation just occurs only at the slow shocks and the X-line where the initial diffusion commences. Such a treatment applied by *Semenov* and his co-workers is based on considerations of mathematical simplicity in order to find analytic solutions to the problem.

This scenario is quite like that of the multiple X-line reconnection due to the tearing mode in the stage when one

X-line eventually becomes dominant and two reconnection outflows in opposite direction emanate from it. One difference is that the dissipation occurs everywhere in the sheet undergoing tearing, and the dominant X-line develops in a self-consistent fashion from many X-lines during the process (e.g., see *Fu and Lee* [1985]). But the dominant X-line in the Petschek-type reconnection is fixed artificially from the very beginning. Another difference comes from our understanding of the dissipation mechanisms in the process. In the tearing mode version, the dissipation occurs in the whole current sheet as a result of the plasma turbulence caused by the instability. In the Petschek version, on the other hand, in addition to the diffusion region, the slow shocks play the main role in the energy conversion. These two approaches should be physically equivalent. Comparing the arguments and discussions of *Forbes and Malherbe* [1991] and *Priest and Forbes* [2000, pp. 391–393] on the same results from the numerical experiment of reconnection in the two-ribbon flare process seems to be suggestive of such an equivalence. But rigorous studies of this equivalence are not yet available due to mathematical difficulties.

In addition to the interior structure of the reconnecting current sheets, it is also necessary to pay attention to the environment outside the sheet and its possible impacts on the energy conversion process. In discussions of magnetotail versus corona reconnection, one topic that has come up repeatedly is whether there is any evidence for the strong increases in Alfvén speed at the Sun as one moves normal to the reconnecting sheet. The gradients are large in the Earth’s tail with Alfvén speeds of < 100 km s $^{-1}$ in the central plasma sheet where reconnection commences, but increasing to > 1000 km s $^{-1}$ over 100 to 1000 km distant in the outer plasma sheet and lobes. This strong gradient is believed to be the source of the “explosive” appearance of magnetotail reconnection as first the low Alfvén speed flux tubes in the central plasma sheet reconnect followed later by the high Alfvén speed lobe flux tubes (e.g., see *Hesse et al.* [1996]).

In principle, fast reconnection in the solar corona also occurs during the explosive event, like flares, in the current sheet where a large gradient of Alfvén speed exists in the direction normal to the sheet. This is represented indirectly by the dramatic change in plasma β from well below unity outside the sheet to around unity inside the sheet (e.g., see *Ko et al.* [2003]), and by the significant difference between the inflow and the outflow speeds of the plasma measured around the sheet developed in an eruption (e.g., see *Lin et al.* [2005]). Unlike the geomagnetic tail sheet in the “explosive” stage, however, the coronal sheet in the “explosive” phase does not exist beforehand, but forms and develops during the eruptive process. So the strong gradient of the Alfvén speed across the CME/flare sheet is not the very source of the “explosive” appearance of reconnection. Instead the CME/flare current sheet forms as the closed magnetic field is severely stretched by the eruption, separating magnetic field lines of opposite polarity, and the temporal vacuum around the sheet quickly brings these field lines and plasma into the sheet driving reconnection to occur (e.g., see *Lin et al.* [2003]). In this process it is not necessarily the magnetic field of the low Alfvén speed that reconnects before that of high Alfvén speed. But it is true that the Alfvén speed inside the sheet is low compared to that outside (e.g., see *Forbes and Malherbe* [1991]).

5. Summary

As an efficient energy conversion process in magnetized plasma environments, magnetic reconnection takes place in

the solar atmosphere, magnetosphere, laboratory plasmas, and in other astrophysical contexts. Here we have emphasized the solar and magnetospheric context because, so far, these are the only two places where the magnetic reconnection process on the large scale can be observed or detected directly. We compared their morphological features and physical properties, discussed the reconnection process as a means of energy conversion and detailed the observational consequences. This comparative study reveals several pieces of important information that help us understand the physics related to the large scale energy conversion and release processes that may occur in the magnetized plasma environments on other objects in the universe.

The main results we deduced from the comparison performed in the present work are summarized as follows:

1. In both solar atmosphere and magnetosphere, reconnection slowly sends the magnetic flux and energy from the region of low V_A and high β to that of high V_A and low β , then the magnetic energy stored in the latter is quickly released by reconnection causing violent eruptions.

2. Energy conversion through magnetic reconnection in both environments takes place in current sheets. These sheets form as a result of the interaction between the solar wind and the geomagnetic field in the magnetosphere, in one case; and in the corona, they develop when the closed magnetic field lines are stretched by the eruption.

3. Reconnection takes place in the current sheet when the sheet becomes thin enough. In the Earth's magnetotail, measurements by Geotail and Cluster indicate that reconnection does not take place until the sheet has thinned to the point where not only the ions have become "demagnetized", but embedded electron scale effects become important to provide the necessary dissipation as well. In the solar CME/flare, it was also shown that reconnection commenced when two magnetic fields of opposite polarity were pushed against each other, which implies that the sheet between the two fields got thinned (e.g., see *Lin et al.* [2005]). At present, it is not clear how thin the sheet should be, but it is usually believed that reconnection begins as a result of the tearing mode when the sheet length exceeds $\sim 2\pi$ times its thickness (e.g., see *Furth et al.* 1963; *Priest and Forbes* [2000]).

4. Huge difference between the two contexts in length scale and in magnetic field strength yields significant difference between them in the absolute values of both amount and rate of energy release during eruptions. But if we consider a dimensionless energy release rate, M_A , namely the relative rate of reconnection, then we found that the eruptive processes in the different environments typically take place at the same rate. This implies that the energy conversion via reconnection on other objects in the universe are quite likely to occur at the same M_A as on the Sun and on the Earth.

5. The most magnificent morphological features observed (detected) in the solar eruption (substorms) are the plasma blobs (plasmoids) flowing along the respective reconnecting current sheets. The flow of the blob observed in several solar eruptions was identified with the reconnection outflow, and was used to deduce the Alfvén speed in the corona.

6. The blob flows in both directions are well observed, but those propagating away from the Sun in solar eruptions and tailward in substorms can be recognized more easily than those towards the Sun and the Earth. The closed field lines below the current sheet produced by magnetic reconnection is the reason responsible for such a discrimination of the plasma flow behaviors in both contexts.

7. Plasma blobs or plasmoids could be identified with either the magnetic islands caused by the tearing mode instability (turbulence) or the reconnection outflow regions surrounded by the slow mode shocks in the Petschek-type reconnection process. In both cases, magnetic reconnection dissipates the magnetic field in a fairly efficient fashion. The high efficiency of the energy conversion results from the hyper-resistivity in the former case, and from the slow mode shocks in the latter case. More work in theory, observation, and numerical experiments are expected to shed light on this issue.

Acknowledgments. We thank N. Crooker for valuable comments and suggestions. We are also grateful for both referee's valuable comments and suggestions that help improve this paper. JL thanks ISSI (International Space Science Institute, Bern) for the hospitality provided to the members of the team on the Role of Current Sheets in Solar Eruptive Events where some of the ideas presented in this work have been discussed. JL's work at YNAO was supported by the Ministry of Science and Technology of China under the Program 973 grant 2006CB806303, by the National Natural Science Foundation of China under the grant 40636031, and by the Chinese Academy of Sciences under the grant KJCX2-YW-T04 to YNAO, and he was supported by NASA grant NNX07AL72G when visiting Cfa. SRC acknowledges support from NASA grant NNG04GE77G. CJF acknowledges support from NASA grants NNX08AD11G, NNG05GC75G, and NNG06GDD41G. *SOHO* is a joint mission of the European Space Agency and the US National Aeronautics and Space Administration.

References

- Ambrosiano, J., W. H. Matthaeus, M. L. Goldstein, D. Plante (1988), Test particle acceleration in turbulent reconnecting magnetic fields, *J. Geophys. Res.*, *93*, 14383–14400.
- André, M., A. Vaivads, S. C. Buchert, A. N. Fazakerley, and A. Lahiff (2004), Thin electron-scale layers at the magnetopause, *Geophys. Res. Lett.*, *31*, CiteID L03803.
- Angelopoulos, V., W. Baumjohann, C. F. Kennel, F. V. Coroniti, M. G. Kivelson, R. Pellat, R. J. Walker, H. Lhr, and G. Paschmann (1992), Bursty bulk flows in the inner central plasma sheet, *J. Geophys. Res.*, *97*, 4027–4039.
- Asai, A., T. Yokoyama, M. Shimojo, and K. Shibata (2004), Downflow Motions Associated with Impulsive Nonthermal Emissions Observed in the 2002 July 23 Solar Flare, *Astrophys. J.*, *605*, L77–L80.
- Aschwanden, M. J. (2005), *Physics of the Solar Corona. An Introduction with Problems and Solutions*. Springer: New York.
- Baker, D. N., R. C. Anderson, R. D. Zwickl, and J. A. Slavin (1987), Average plasma and magnetic field variations in the Distant magnetotail associated with Near-Earth substorm effects, *J. Geophys. Res.*, *92*, 71–81.
- Baker, D. N., T. A. Fritz, R. L. McPherron, D. H. Fairfield, Y. Kamide, and W. Baumjohann (1985), Magnetotail energy storage and release during the CDAW 6 substorm analysis intervals, *J. Geophys. Res.*, *90*, 1205–1216.
- Baker, D. N., T. I. Pulkkinen, V. Angelopoulos, V. Baumjohann, R. L. McPherron (1996), Neutral line model of substorms: Past results and present view, *J. Geophys. Res.*, *101*, 12975–13010.
- Baumjohann, W., G. Paschmann, and C. A. Cattell (1989), Average plasma properties of the central plasma sheet, *J. Geophys. Res.*, *94*, 6597–6606.
- Baumjohann, W., G. Paschmann, and H. Lhr (1990), Characteristics of high-speed ion flows in the plasma sheet, *J. Geophys. Res.*, *95*, 38013809.
- Bemporad, A., G. Poletto, S. T. Suess, Y.-K. Ko, N. A. Schwadron, H. A. Elliott, and J. C. Raymond (2006), Current Sheet Evolution in the Aftermath of a CME Event *Astrophys. J.*, *638*, 1110–1128.
- Bhattacharjee, A. and Y. Yuan (1995), Self-Consistency Constraints on the Dynamo Mechanism, *Astrophys. J.*, *638*, 739.
- Biernat, H. K., M. F. Heyn, and V. S. Semenov (1987), Unsteady Petschek reconnection, *J. Geophys. Res.*, *92*, 3392–3396.
- Birn, J., J. F. Drake, M. A. Shay, B. N. Rogers, R. E. Denton, M. Hesse, and other 5 co-authors (2001), Geospace Environmental Modeling (GEM) Magnetic Reconnection Challenge, *J. Geophys. Res.*, *106*(A3), 3715–3719, 2001.

- Birn, J., T. G. Forbes, and M. Hesse (2006), Stability and Dynamic Evolution of Three-Dimensional Flux Rope, *Astrophys. J.*, *645*, 732–741.
- Birn, J., T. G. Forbes, and Schindler (2003), Models of Three-Dimensional Flux Rope, *textitAstrophys. J.*, *588*, 578–585.
- Birn, J., and E. R. Priest (2007), *Reconnection of Magnetic Fields: MHD and Collisionless Theory and Observations* (Cambridge Univ. Press, Boston).
- Birn, J., J. Raeder, Y. L. Wang, R. A. Wolf, and M. Hesse (2004), On the propagation of bubbles in the geomagnetic tail, *Ann. Geophys.*, *22*, 1773–1786.
- Burlaga, L. F. (1988), Magnetic clouds: Constant alpha force-free configurations, *J. Geophys. Res.*, *93*, 7217–7224.
- Burlaga, L. F., E. Sittler, F. Mariani, and R. Schwenn (1981), Magnetic loop behind an interplanetary shock: Voyager, Helios and IMP 8 observations, *J. Geophys. Res.*, *86*, 6673–688.
- Carmichael, H. (1964), A process for flares, in *The Physics of Solar Flares*, ed. W. N. Hess (NASA SP-50; Washington, DC: NASA), 451–456.
- Cassak, P. A., J. F. Drake, and M. A. Shay (2006), A Model for Spontaneous Onset of Fast Magnetic Reconnection, *Astrophys. J.*, *644*, L145–L148.
- Cassak, P. A., D. J. Mullan, and M. A. Shay (2008), From Solar and Stellar Flares to Coronal Heating: Theory and Observations of How Magnetic Reconnection Regulates Coronal Conditions, *Astrophys. J.*, *676*, L69–L72.
- Ciaravella, A., J. C. Raymond, J. Li, P. Reiaer, L. D. Gardner, Y.-K. Ko, and S. Fineschi (2002), Elemental Abundances and Post-Coronal Mass Ejection Current Sheet in a Very Hot Active Region, *Astrophys. J.*, *575*, 1116–1128.
- Coleman, P. J., Jr. (1968), Turbulence, Viscosity, and Dissipation in the Solar-Wind Plasma, *Astrophys. J.*, *153*, 371–388.
- Coppi, B. (1965), Role of Plasma Instabilities in Auroral Phenomena, *Nature*, *201*, 998.
- Coppi, B., G. Laval, and R. Pellat (1966), Dynamics of the geomagnetic tail, *Phys. Rev. Lett.*, *16*(26), 1207–1210.
- Cowley, S. W. H. (1980), Plasma populations in a simple open model magnetosphere, *Space Sci. Rev.*, *26*, 217–274.
- Cranmer, S. R., A. A. van Ballegoijen, and R. J. Edgar (2007), Self-consistent Coronal Heating and Solar Wind Acceleration from Anisotropic Magnetohydrodynamic Turbulence, *Astrophys. J. (Supp.)*, *171*, 520–551.
- Démoulin, P., J. C. Hénoux, E. R. Priest, and C. H. Malherbe (1996), Quasi-Separatrix layers in solar flares. I. Method, *Astron. Astrophys.*, *308*, 643–655.
- Dmitruk, P., and W. H. Matthaeus (2006), Test particle acceleration in three-dimensional Hall MHD turbulence, *J. Geophys. Res.*, *111*, A12110.
- Dmitruk, P., W. H. Matthaeus, and N. Seenu (2004), Test Particle Energization by Current Sheets and Nonuniform Fields in Magnetohydrodynamic Turbulence, *Astrophys. J.*, *617*, 667–679.
- Drake, J. F., M. Swisdak, K. M. Schoeffler, B. N. Rogers, and S. Kobayashi (2006), Formation of secondary islands during magnetic reconnection, *Geophys. Res. Lett.*, *33*, CiteID L13105.
- Dungey, J. W. (1953), Conditions for the occurrence of electrical discharges in astrophysical systems, *Phil. Mag.*, *44*, 725–738.
- Dungey, J. W. (1958), The neutral point discharge theory of solar flare. A reply to Cowling's criticism, in *Electromagnetic Phenomena in Cosmical Physics*, IAU Symp. 6, ed. B. Lehnert (Cambridge Univ. Press), 135–140.
- Dungey, J. W. (1961), Interplanetary Magnetic Field and the Auroral Zones, *Phys. Rev. Lett.*, *6* (2), 47–48.
- Eastwood, J. P., T. D. Phan, F. S. Mozer, M. A. Shay, M. Fujimoto, A. Rentinò, and another 4 co-authors (2007), Multi-point observations of the Hall electromagnetic field and secondary island formation during magnetic reconnection, *J. Geophys. Res.*, *112*(A6), CiteID A06235.
- Eastwood, J. P., D. G. Sibeck, J. A. Slavin, M. L. Goldstein, B. Lavraud, M. Sitnov, S. Imber, A. Balogh, E. A. Lucack, and I. Dandouras (2005), Observations of multiple X-line structure in the Earth's magnetotail current sheet: A Cluster case study, *Geophys. Res. Lett.*, *32*, L11105, doi:10.1029/2005GL022509.
- Einaudi, G., P. Boncinelli, R. B., Dahlburg, and J. T. Karpen, (1999), Formation of the slow solar wind in a coronal streamer, *J. Geophys. Res.*, *104*, 521–534.
- Einaudi, G., S. Chibbaro, R. B. Dahlburg, and M. Velli (2001), Plasmoid Formation and Acceleration in the Solar Streamer Belt, *Astrophys. J.*, *547*, 1167–1177.
- Elphic, R. C., T. G. Onsager, M. F. Thomsen, and J. T. Gosling (1995), Nature and location of the source of plasma sheet boundary layer ion beams, *J. Geophys. Res.*, *100*, 1857–1869.
- Emslie, A. G., E. P. Kontar, S. Krucker, and R. P. Lin (2003), RHESSI Hard X-Ray Imaging Spectroscopy of the Large Gamma-Ray Flare of 2002 July 23, *Astrophys. J.*, *595*, L107–L110.
- Erickson, G. M., and R. A. Wolf (1980), Is steady convection possible in the earth's magnetotail?, *Geophys. Res. Lett.*, *7*, 897–900.
- Eriksson, S., M. Øiereoset, D. N. Baker, C. Mouikis, A. Vaivads, M. W. Dunlop, H. Reme, R. E. Ergun, and A. Balogh (2004), Walén and slow-mode shock analyses in the near-Earth magnetotail in connection with a substorm onset on 27 August 2001 (2004), *J. Geophys. Res.*, *109*, A10212, doi:10.1029/2004JA010534.
- Farrugia, C. J., M. P. Freeman, L. F. Burlaga, R. P. Lepping, and K. Takahashi (1993a), The Earth's magnetosphere under continued forcing: Substorm activity during the passage of an interplanetary magnetic cloud, *J. Geophys. Res.*, *98*, 7657.
- Farrugia, C. J., L. F. Burlaga, V. Osherovich, I. G. Richardson, M. P. Freeman, R. P. Lepping, and A. Lazarus (1993b), A study of an expanding interplanetary magnetic cloud and its interaction with the Earth's magnetosphere: The interplanetary aspect, *J. Geophys. Res.*, *98*, 7621.
- Farrugia, C. J., I. G. Richardson, L. F. Burlaga, V. A. Osherovich, and R. P. Lepping (1993c), Simultaneous observations of Solar MeV particles in a magnetic cloud and in the Earth's northern tail lobe: Implications for the global field line topology of magnetic clouds and entry of solar particles into tail lobe during cloud passage, *J. Geophys. Res.*, *98*, 15,497.
- Farrugia, C. J., D. J. Southwood, and S. W. H. Cowley, Observations of flux transfer events (1988), *Adv. Space Res.*, *Vol 8, No. 9-10*, 249.
- Farrugia, C. J., B. Vasquez, R. B. Torbert, I. G. Richardson, L. F. Burlaga, H. K. Biernat, and other 8 co-authors (2001), A reconnection layer associated with a magnetic cloud, *Adv. Space Res.*, *28, No. 5*, 759.
- Feldman, W. C., D. N. Baker, S. J. Bame, J. Birn, J. T. Gosling, E. W. Hones, Jr., and S. J. Schwartz (1985), Slow-mode shocks - A semipermanent feature of the distant geomagnetic tail, *J. Geophys. Res.*, *90*, 233–240.
- Feldman, W. C., S. R. Habbal, G. Hoogeveen, and Y.-M. Wang (1997), Experimental constraints on pulsed and steady state models of the solar wind near the Sun, *J. Geophys. Res.*, *102*, 26905–26918.
- Feldman, W. C., S. J. Schwartz, S. J. Baem, D. N. Baker, J. Birn, J. T. Gosling, E. W. Hones, Jr., D. J. McComas, J. A. Slavin, E. J. Smith, and R. D. Zwickl (1984), Evidence for slow-mode shocks in the deep geomagnetic tail, *Geophys. Res. Lett.*, *11*, 599–602.
- Fisk, L., and N. A. Schwadron (2001), The Behavior of the Open Magnetic Field of the Sun, *Astrophys. J.*, *560*, 425–438.
- Forbes, T. G. (2000), A review on the genesis of coronal mass ejections, *J. Geophys. Res.*, *105*, 23153–23166.
- Forbes, T. G. (2007), The Origin of Solar Eruptions, *AIP Conf. Proc.*, *934*, 13–21.
- Forbes, T. G., and L. W. Acton (1996), Reconnection and Field Line Shrinkage in Solar Flares, *Astrophys. J.*, *459*, 330.
- Forbes, T. G., and P. A. Isenberg (1991), A catastrophe mechanism for coronal mass ejections, *Astrophys. J.*, *373*, 294–307.
- Forbes, T. G., and J. Lin (2000), What can we learn about reconnection from coronal mass ejections?, *J. Atmos. Sol.-Terr. Phys.*, *62*, 1499.
- Forbes, T. G., and J. M. Malherbe (1991), A numerical simulation of magnetic reconnection and radiative cooling in line-tied current sheets, *Sol. Phys.*, *135*, 361–391.
- Fu, Z., and L. Lee (1985), Simulation of multiple X-line reconnection at the dayside magnetopause, *Geophys. Res. Lett.*, *12*(No. 5), 291–294.
- Furth, H. P., J. Killeen, and M. N. Rosenbluth (1963), Finite-Resistivity Instabilities of a Sheet Pinch, *Phys. Fluids*, *6*, 459–484.
- Goldstein, M. L., D. A. Roberts, and W. H. Matthaeus (1995), Magnetohydrodynamic Turbulence In The Solar Wind, *Annual Reviews Astron. Astrophys.*, *33*, 283–326.

- Gosling, J. T. (2007), Observations of Magnetic Reconnection in the Turbulent High-Speed Solar Wind, *Astrophys. J.*, *671*, L73-L76.
- Gosling, J. T., S. Eriksson, R. M. Skoug, D. J. McComas and R. J. Forsyth (2006), Petschek-Type Reconnection Exhausts in the Solar Wind Well beyond 1 AU: Ulysses, *Astrophys. J.*, *644*, 613-621.
- Gosling, J. T., R. M. Skoug, D. J. McComas, and C. W. Smith (2005), Magnetic disconnection from the Sun: Observations of a reconnection exhaust in the solar wind at the heliospheric current sheet, *Geophys. Res. Lett.*, *32*, L05105.
- Hesse, M., and J. Birn (1991), Plasmoid evolution in an extended magnetotail, *J. Geophys. Res.*, *96*, 5683-5696.
- Hesse, M., J. Birn, D. N. Baker, and J. A. Slavin (1996), MHD simulations of the transition of magnetic reconnection from closed to open field lines, *J. Geophys. Res.*, *101*, 10805-10816.
- Hesse, M. and M. G. Kivelson (1998), The formation and structure of flux ropes in the magnetotail, *AGU Monograph 105*, eds A. Nishida and S. W. H. Cowley, pp. 139.
- Hada, T., C. F. Kennel (1985), Nonlinear evolution of slow waves in the solar wind, *J. Geophys. Res.*, *90*, 531-535.
- Ho, C. M., and B. T. Tsurutani (1997), Distant tail behavior during high speed solar wind streams and magnetic storms, *J. Geophys. Res.*, *102*, 14165-14176.
- Hollweg, J. V. (1986), Transition region, corona, and solar wind in coronal holes, *J. Geophys. Res.*, *91*, 4111-4125.
- Hones, E. W., Jr. (1977), Substorm Processes in the Magnetotail: Comments on 'On Hot Tenuous Plasmas, Fireballs, and Boundary Layers in the Earth's Magnetotail' by L. A. Frank, K. L. Ackerson, and R. P. Lepping, *J. Geophys. Res.*, *82*, 5633-5640.
- Huang, C.-S., G. D. Reeves, J. E. Borovsky, R. M. Skoug, Z. Y. Pu, and G. Le (2003), Periodic magnetospheric substorms and their relationship with solar wind variations, *J. Geophys. Res.*, *108*, 1255, doi:10.1029/2002JA009704.
- Heyn, M. F., H. K. Biernat, R. P. Rijnbeek, and V. S. Semenov (1988), The structure of reconnection layers, *J. Plasma Phys.*, *40*, 235.
- Innes, D. E., D. E. McKenzie, and T. Wang (2003) SUMER spectral observations of post-flare supra-arcade inflows, *Sol. Phys.*, *217*, 247-265.
- Kinney, R., J. C. McWilliams, T. Tajima (1995), Coherent structures and turbulent cascades in two-dimensional incompressible magnetohydrodynamic turbulence, *Phys. Plasmas*, *2*, 3623-3639.
- Klein, L. W., and L. F. Burlaga (1982), Interplanetary magnetic clouds at 1 AU, *J. Geophys. Res.*, *87*, 613-624.
- Klimchuk J. A. (2001), Theory of coronal mass ejections, in *Space Weather (AGU Monograph)*, eds. P. Song, G. Siscoe, and H. Singer, 143-157.
- Ko, Y., J. C. Raymond, J. Lin, G. Lawrence, J. Li, and A. Fludra (2003), Dynamical and Physical Properties of a Post-Coronal Mass Ejection Current Sheet, *Astrophys. J.*, *594*, 1068-1084.
- Kohl, J. L., G. Noci, S. R. Cranmer, and J. C. Raymond (2006), Ultraviolet spectroscopy of the extended solar corona, *Astron. Astrophys. Rev.*, *13*, 31-157.
- Kohl, J. L., G. Noci, E. Antonucci, G. Tondello, M. C. E. Huber, and another 21 co-authors (1997), First Results from the SOHO Ultraviolet Coronagraph Spectrometer, *Sol. Phys.* *175*, 613-644.
- Kopp, R. A., and G. W. Pneuman (1976), Magnetic reconnection in the corona and the loop prominence phenomenon, *Sol. Phys.* *50*, 85-98.
- Krauss-Varban, D., and N. Omidi (1995), Large-scale hybrid simulations of the magnetotail during reconnection, *Geophys. Res. Lett.*, *22*, 3271-3274.
- Lapenta, G., and D. A. Knoll (2005), Effect of a Converging Flow at the Streamer Cusp on the Genesis of the Slow Solar Wind, *Astrophys. J.*, *624*, 1049-1056.
- Lazarian, A., and E. T. Vishniac (1999), Reconnection in a Weakly Stochastic Field, *Astrophys. J.*, *517*, 700-718.
- Leamon, R. J., W. H. Matthaeus, C. W. Smith, G. P. Zank, D. J. Mullan, and S. Oughton (2000), MHD-driven Kinetic Dissipation in the Solar Wind and Corona, *Astrophys. J.*, *537*, 1054-1062.
- Lee, L. C. (1990), Time-dependent magnetic reconnection: Two- and three-dimensional MHD simulations, *Comp. Phys. Comm.*, *59*, 163-174.
- Lee, L. C., and Z. F. Fu (1985), A Theory of Magnetic Flux Transfer at the Earth's Magnetopause, *Geophys. Res. Lett.*, *12*(No. 2), 105-108.
- Lee, L. C., and Z. F. Fu (1986), Multiple X line reconnection. I - A criterion for the transition from a single X line to a multiple X line reconnection, *J. Geophys. Res.*, *91*, 6807-6815.
- Lee, L. C., Z. F. Fu, and S.-I. Akasofu (1985), A simulation Study of Forced Reconnection Processes and Magnetospheric Storms and Substorms, *J. Geophys. Res.*, *90*(A11), 10896-10910.
- Lepping, R. P., J. A. Jones, and L. F. Burlaga (1990), Magnetic field structure of interplanetary magnetic clouds at 1 AU, *J. Geophys. Res.*, *95*(A8), 11957-11965.
- Lin, J. (2002), Energetics and Propagation of Coronal Mass Ejections in Different Plasma Environments, *Chin. J. Astron. Astrophys.* *2*, 539-556.
- Lin, J., and T. G. Forbes (2000), Effects of reconnection on the coronal mass ejection process, *J. Geophys. Res.*, *105*, 2375-2392.
- Lin, J., T. G. Forbes, E. R. Priest, and T. N. Bungey (1995a), Models for the Motions of Flare Loops and Ribbons, *Solar Phys.*, *159*, 275-299.
- Lin, J., Y.-K. Ko, L. Sui, J. C. Raymond, G. A. Stenborg, Y. Jiang, S. Zhao, and S. Mancuso (2005), Direct Observations of the Magnetic Reconnection Site of an Eruption on 2003 November 18, *Astrophys. J.*, *622*, 1251-1264.
- Lin, J., J. Li, T. G. Forbes, Y.-K. Ko, J. C. Raymond, and A. Vourlidas (2007), Features and Properties of Coronal Mass Ejection/Flare Current Sheets, *Astrophys. J.*, *658*, L123-L126.
- Lin, J., J. C. Raymond, and A. A. van Ballegoijen (2004), The Role of Magnetic Reconnection in the Observable Features of Solar Eruptions, *Astrophys. J.*, *602*, 422-435.
- Lin, J., R. P. Rijnbeek, V. S. Semenov, M. T. Kiendl, and H. K. Biernat (1995b), Analysis of Petschek-type reconnection in a Y-type magnetic field distribution, *Planet. Space Sci.*, *43*, 923-938.
- Lin, J., W. Soon, and S. L. Baliunas (2003), Theories of solar eruptions: a review, *New Astron. Rev.* *47*, 53-84.
- Litvinenko, Y. (1996), Particle Acceleration in Reconnecting Current Sheets with a Nonzero Magnetic Field, *Astrophys. J.*, *462*, 997.
- Loureiro, N. F., A. A. Schekochihin, S. C. Cowley (2007), Instability of current sheets and formation of plasmoid chains, *Phys. Plasma*, *14*(10), 100703.
- Lundquist, S. (1950), Magnetohydrostatic fields, *Ark. Fys.* *2*, 361.
- Markovskii, S. A., B. J. Vasquez, C. W. Smith, and J. V. Hollweg (2006), Dissipation of the Perpendicular Turbulent Cascade in the Solar Wind, *Astrophys. J.*, *639*, 1177-1185.
- Martens, P. C. H., and N. P. M. Kuin (1989), A circuit model for filament eruptions and two-ribbon flares, *Sol. Phys.*, *122*, 263-302.
- Matthaeus, W. H., G. P. Zank, S. Oughton, D. J. Mullan, and P. Dmitruk (1999), Coronal Heating by Magnetohydrodynamic Turbulence Driven by Reflected Low-Frequency Waves, *Astrophys. J.*, *523*, L93-L96.
- McKenzie, D. E. (2000), Supra-arcade Downflows in Long-Duration Solar Flare Events, *Sol. Phys.*, *195*, 381-399.
- McKenzie, D. E., and H. S. Hudson (1999), X-Ray Observations of Motions and Structure above a Solar Flare Arcade, *Astrophys. J.*, *519*, L93-L96.
- McPherron, R. L. (1991), Physical processes producing magnetospheric substorms and magnetospheric storms, in *Geomagnetism*, *4*, Academic Press.
- McPherron, R. L., C. T. Russell, and M. P. Aubry (1973), Satellite studies of magnetospheric substorms on August 15, 1968. 9. Phenomenological model for substorms, *J. Geophys. Res.*, *78*, 3131-3149.
- Mininni, P. D., A. G. Pouquet, D. C. Montgomery (2006), Small-Scale Structures in Three-Dimensional Magnetohydrodynamic Turbulence, *Phys. Rev. Lett.*, *97*, 244503.
- Mullan, D. J. (1990), Sources of the solar wind - What are the smallest-scale structures?, *Astron. Astrophys.*, *232*, 520-535.
- Moldwin, M. B., S. Ford, R. P. Lepping, J. Slavin and A., Szabo (2000), Small-scale magnetic flux ropes in the solar wind, *Geophys. Res. Lett.*, *27*, 57-60, 2000.
- Moldwin, M. B., and W. J. Hughes (1994), Observations of Earthward and tailward propagating flux rope plasmoids: Expanding the plasmoid model of geomagnetic substorms, *J. Geophys. Res.*, *99*, 183-198.

- Murata, T., H. Matsumoto, H. Kojima, A. Fujita, T. Nagai, T. Yamamoto, R. R. Anderson (1995), Estimation of tail reconnection lines by AKR onsets and plasmoid entries observed with GEOTAIL spacecraft, *Geophys. Res. Lett.*, *22*, No. 14, 1849.
- Nagai, T., I. Shinohara, M. Fujimoto, M. Hoshino, Y. Saito, and T. Mukai (2001), Geotail observations of the Hall current system: Evidence of magnetic reconnection in the magnetotail, *J. Geophys. Res.*, *105*, 25,929–25,949.
- Ness, N. F. (1965), The Earth's magnetic tail, *J. Geophys. Res.*, *70*(13), 2989–3005.
- Nishida, A., T. Mukai, T. Yamamoto, and S. Kokubun (1998), Plasma sheet beyond the distant tail, *Geophys. Res. Lett.*, *25*, 4055–4058.
- Nishida, A., T. Yamamoto, K. Tsuruda, H. Hayakawa, A. Matsumoto, S. Kokubun, M. Nakamura, and H. Kawano (1994), Classification of the tailward drifting magnetic structures in the distant tail, *Geophys. Res. Lett.*, *21*, 2947–2950.
- Øieroset, M., T. D. Phan, R. P. Lin, and B. U. Ö. Sonnerup (2000), Walén and variance analyses of high-speed flows observed by Wind in the midtail plasma sheet: Evidence for reconnection, *J. Geophys. Res.*, *105*, 25247–25264.
- Øieroset, M., T. D. Phan, M. Fujimoto, R. P. Lin and R. P. Lepping (2001), *In situ* detection of collisionless reconnection in the Earth's magnetotail, *Nature*, *412*, 414.
- Parker, E. N. (1957), Sweet's Mechanism for Merging Magnetic Fields in Conducting Fluids, *J. Geophys. Res.*, *62*, 509–520.
- Parker, E. N. (1963), The Solar-Flare Phenomenon and the Theory of Reconnection and Annihilation of Magnetic Fields, *Astrophys. J. (Supp.)*, *8*, 177–211.
- Paschmann, G., I. Papamastorakis, W. Baumjohann, N. Skopke, C. W. Carlson, B. U. Ö. Sonnerup, and H. Lühr (1986), The magnetopause for large magnetic shear: AMPTE/IRM observations, *J. Geophys. Res.*, *91*, 11,099–11,115.
- Paschmann, G., B. U. Ö. Sonnerup, I. Papamastorakis, N. Skopke, G. Haerendel, S. J. Bame, J. R. Asbridge, J. T. Gosling, C. T. Russell, and R. C. Elphic (1979), Plasma acceleration at the Earth's magnetopause: Evidence for reconnection, *Nature*, *282*, 243.
- Paschmann G., S. J. Schwartz, C. P. Escoubet, and S. Haaland, *Outer Magnetospheric Boundaries: Cluster Results*, Berlin: Springer, 2005.
- Petschek, H. E. (1964), Magnetic field annihilation, in *The Physics of Solar Flares*, edited by W. N. Hess, NASA, *Spec. Publ. SP-50*, 425–439.
- Phan, T. D., L. M. Kistler, B. Klecker, G. Haerendel, G. Paschmann, B. U. Ö. Sonnerup, and other 14 co-authors (2000), Extended magnetic reconnection at the Earth's magnetopause from detection of bi-directional jets, *Nature*, *404*, 848–850.
- Pneuman, G. W. (1983), Ejection of magnetic fields from the sun - Acceleration of a solar wind containing diamagnetic plasmoids, *Astrophys. J.*, *265*, 468–482.
- Pneuman, G. W. (1986), Driving mechanisms for the solar wind, *Space Sci. Rev.*, *43*, 105–138.
- Poletto, G., and R. A. Kopp (1986), in *The lower atmosphere of solar flares*, Proceedings of the Solar Maximum Mission Symposium, Sunspot, NM, Aug. 20–24, 1985 (A87-26201 10-92), 453–465.
- Priest, E. R. (1982), *Solar Magnetohydrodynamics*. Reidel, Hingham, MA.
- Priest, E. R. (1985), The magnetohydrodynamics of current sheets, *Rep. Prog. Phys.*, *48*, 955–1090.
- Priest, E. R., and T. G. Forbes (2000), *Magnetic Reconnection: MHD Theory and Applications*, New York: Cambridge University Press.
- Priest, E. R., and T. G. Forbes (2002), The magnetic nature of solar flares, *A&A Rev.* *10*, 313–377.
- Pritchett, P. L., and F. V. Coroniti (1990), Plasma sheet convection and the stability of the magnetotail, *Geophys. Res. Lett.*, *17*, 2233–2236.
- Pritchett, P. L., F. V. Coroniti, R. Pellat, and H. Karimabadi (1991), Collisionless reconnection in two-dimensional magnetotail equilibria, *J. Geophys. Res.*, *96*, 11523–11538.
- Pudovkin, M. I., and V. S. Semenov (1985), Magnetic field reconnection theory and the solar wind-magnetosphere interaction: A review, *Space Sci. Rev.*, *41*, 1.
- Qiu, J., H. Wang, C. Z. Cheng, and D. E. Gary (2004), Magnetic Reconnection and Mass Acceleration in Flare-Coronal Mass Ejection Events, *Astrophys. J.*, *604*, 900–905, (2004).
- Raymond, J. C., A. Ciaravella, D. Dobrzycka, L. Strachan, Y.-K. Ko, M. Uzzo, N.-E. Raouafi (2003), Far-Ultraviolet Spectra of Fast Coronal Mass Ejections Associated with X-Class Flares, *Astrophys. J.*, *597*, 1106–1117.
- Raymond, J. C., J. L. Kohl, G. Noci, E. Antonucci, G. Tondello, and another 22 co-authors (1997), Composition of Coronal Streamers from the SOHO Ultraviolet Coronagraph Spectrometer, *Sol. Phys.* *175*, 645–665.
- Reeves, K. K., T. B. Guild, W. J. Hughes, K. E. Korreck, J. Lin, J. C. Raymond, S. Savage, N. A. Schwadron, H. E. Spence, D. F. Webb, and M. Wiltberger (2008), Post-Eruptive Phenomena in CMEs and Substorms - Indicators of A Universal Process?, *J. Geophys. Res.*, , in press.
- Rentiniò, A., D. Sundkvist, A. Vaivads, F. Mozer, M. André, and C. J. Owen (2007), In situ evidence of magnetic reconnection in turbulent plasma, *Nat. Phys.*, *3*, 236–238.
- Rijnbeek, R. P., H. K. Biernat, M. F. Heyn, V. S. Semenov, and C. J. Farrugia (1989), The structure of the reconnection layer observed by ISEE 1 on 8 September 1978, *An. Geophys.* *7*, 297–310.
- Riley, P., R. Lionello, Z. Mikić, J. A. Linker, E. Clark, J. Lin, and Y.-K. Ko (2007), “Bursty” Reconnection Following Solar Eruptions: MHD Simulations and Comparison with Observations, *Astrophys. J.*, *655*, 591–597.
- Russell, C. T., and R. C. Elphic (1978), Initial ISEE magnetometer results: magnetopause observations, *Space Sci. Rev.* *22*, 681–715.
- Sandholt, P. E., and C. J. Farrugia (2001), Multipoint observations of substorm intensifications: The high-latitude aurora and electron injections in the inner equatorial plasma sheet, *Geophys. Res. Lett.*, *28*, 3, 483.
- Schindler, K. (1974), A theory of the substorm mechanism, *J. Geophys. Res.*, *79*, 2803–2810.
- Schlüter, A. (1957), Solar radio emission and the acceleration of magnetic-storm particles in H. C. van de Hulst (ed.), *Radio Astronomy*, IAU Symp. 4, Cambridge U. Press, 356.
- Semenov, V. S., I. V. Kubyshkin, V. V. Lebedeva, R. P. Rijnbeek, M. F. Heyn, H. K. Biernat, and C. J. Farrugia (1992), A comparison and review of steady-state and time-varying reconnection, *Plan. Space Sci.* *40*, 63–87.
- Semenov, V. S., and V. V. Lebedeva (1991), A model problem of the reconnection of thin magnetic force tubes in the cusp region, *Geomagn. Aeronomy*, *31*, 785 (AGU translation).
- Seon, J., L. A. Frank, W. R. Parerson, J. D. Scudder, F. V. Coroniti, S. Kokubun, and T. Yamamoto (1996), Observations of slow-mode shocks in Earth's distant magnetotail with the Geotail spacecraft, *J. Geophys. Res.*, *101*, 27383–27398.
- Sergeev, V. A., K. Liou, C.-I. Meng, P. T. Newell, M. Brittnacher, G. Parks, and G. D. Reeves (1999), Development of auroral streamers in association with localized impulsive injections to the inner magnetotail, *Geophys. Res. Lett.*, *26*, 417–420.
- Shay, M. A., J. F. Drake, B. N. Rodgers, and R. E. Denton (2001), Alfvénic collisionless reconnection and the Hall term, *J. Geophys. Res.*, *106*, 3759–3772.
- Shay, M. A., J. F. Drake, and M. Swisdak (2007), Two-Scale Structure of the Electron Dissipation Region during Collisionless Magnetic Reconnection, *Phys. Rev. Lett.*, *99*(15), id. 155002.
- Sheeley, N. R., Jr., J. H. Walters, Y.-M. Wang, and R. A. Howard (1999), Continuous tracking of coronal outflows: Two kinds of coronal mass ejections, *Astrophys. J.*, *579*, 24739–24768.
- Sheeley, N. R., Jr., and Y.-M. Wang (2002), Characteristics of Coronal Inflows, *Astrophys. J.*, *579*, 874–887.
- Sheeley, N. R., Jr., Y.-M. Wang, S. H. Hawley, E. G. Bruechner, K. P. Dere, and another 14 co-authors (1997), Measurements of Flow Speeds in the Corona between 2 and 30 R_{\odot} , *Astrophys. J.*, *484*, 472.
- Sheeley, N. R., Jr., H. P. Warren, and Y.-M. Wang (2004), The Origin of Postflare Loops, *Astrophys. J.*, *616*, 1224–1231.
- Shodun, S., N. Crooker, S. Kahler, R. Fitzenreiter, D. Larson, R. Lepping, G. Siscoe, and J. Gosling (2000), Counterstreaming electrons in magnetic clouds, *J. Geophys. Res.*, *105*(A12), 27261–27268.
- Sibeck, D. G., G. L. Siscoe, J. A. Slavin, E. J. Smith, S. J. Bame, and F. L. Scarf (1984), Magnetotail flux ropes, *Geophys. Res. Lett.*, *11*, 1090–1093.

- Slavin, J. A., C. J. Owen, M. M. Kuznetsova, and M. Hesse (1995), ISEE 3 observations of plasmoids with flux rope magnetic topologies, *Geophys. Res. Lett.*, *22*, 2061–2064
- Slavin, J. A., C. J. Owen, M. W. Dunlop, E. Borälöv, M. B. Moldwin, D. G. Sibeck, and other 8 co-authors (2003), Cluster four spacecraft measurements of small traveling compression regions in the near-tail, *Geophys. Res. Lett.*, *30*(23), 2208, doi:10.1029/2003GL018438.
- Slavin, J. A., Smith, E. J., D. G. Sibeck, et al. (1984), Substorm associated traveling compression regions in the distant tail: ISEE3-Geotail observations, *Geophys. Res. Lett.*, *11*, 657–660.
- Slavin, J. A., E. J. Stern, D. G. Sibeck, B. N. Baker, R. D. Zwickl, and S.-I. Akasofu (1985), An ISSE 3 study of average and substorm conditions in the distant magnetotail, *J. Geophys. Res.*, *90*, 10875–10895.
- Slavin, J. A., E. I. Tanskanen, M. Hesse, C. J. Owen, M. W. Dunlop, S. Imber, E. A. Lucak, A. Balogh, and K.-H. Glassmeier (2005), Cluster observations of traveling compression regions in the near-tail, *J. Geophys. Res.*, *110*, A06207, doi:10.1029/2004JA010878.
- Sonnerup, B. U. Ö. (1979), in *Solar System Plasma Physics, Vol III*, edited by L. T. Lanzerotti, C. F. Kennel, and E. N. Parker, 45–108, North-Holland, New York.
- Sonnerup, B. U. Ö., and B. G. Ledley (1979), Electromagnetic structure of the magnetopause and boundary layer, in *Magnetospheric Boundary Layers*, edited by B. Battrock, p. 401, ESA SP-148, European Space Agency, Paris.
- Sonnerup, B. U. Ö., I. Papamastorakis, G. Paschmann, and H. Luehr (1987), Magnetopause properties from AMPTE/IRM observations of the convection electric field - Method development, *J. Geophys. Res.*, *92*, 12137–12159.
- Sonnerup, B. U. Ö., G. Paschmann, I. Papamastorakis, N. Scopke, G. Haerendel, S. J. Bame, J. R. Asbridge, J. T. Gosling (1981), and C. T. Russell, Evidence for reconnection at the earth's magnetopause, *J. Geophys. Res.*, *86*, 10,049.
- Southwood, D. J., C. J. Farrugia, and M. A. Saunders (1988), What are flux transfer events?, *Planet. Space Sci.*, *36*, 503.
- Strachan, L., R. M. Suleiman, A. V. Panasyuk, D. A. Biesecker, and J. L. Kohl (2002), Empirical Densities, Kinetic Temperatures, and Outflow Velocities in the Equatorial Streamer Belt at Solar Minimum, *Astrophys. J.*, *571*, 1008–1014.
- Strauss, H. R. (1988), Turbulent reconnection, *Astrophys. J.*, *326*, 412–417.
- Sui, L., and G. D. Holman (2004), Evidence for the Formation of a Large-Scale Current Sheet in a Solar Flare, *Astrophys. J.*, *596*, L251–L254.
- Sui, L., G. D. Holman, and B. R. Dennis (2004), Evidence for Magnetic Reconnection in Three Homologous Solar Flares Observed by RHESSI, *Astrophys. J.*, *612*, 546–556.
- Sundaram, A. K., and D. H. Fairfield (1997), Stability of resistive MHD tearing and ballooning modes in the tail current sheet, *J. Geophys. Res.*, *102*, 19913–19926.
- Švestka, Z., and E. W. Cliver (1992), History and basic characteristics of eruptive flares, in *Eruptive Solar Flares*, eds. Z. Švestka, B. V. Jackson, and M. E. Machado. Springer-Verlag: New York, 1–14.
- Švestka, Z., F. Fárnik, H. S. Hudson, and P. Hick (1998), Large-Scale Active Coronal Phenomena in Yohkoh SXT Images IV. Solar Wind Streams from Flaring Active Regions, *Sol. Phys.* *182*, 179–193.
- Sweet, P. A. (1958a), The neutral point theory of solar flares, in *Electromagnetic Phenomena in Cosmical Physics*, IAU Symp. 6, ed. B. Lehnert (Cambridge Univ. Press, London), 123–134.
- Sweet, P. A. (1958b), The production of high-energy particles in solar flares, *Nuovo Cimento Suppl.*, *8*, Ser. X, 188–196.
- Tamano, T. (1991), A plasmoid model for the solar wind, *Sol. Phys.* *134*, 187–201.
- Tu, C.-Y., and E. Marsch (1995), MHD structures, waves and turbulence in the solar wind: Observations and theories, *Space Sci. Rev.*, *73*, 1–210.
- Uzdensky, D. A. (2007), The Fast Collisionless Reconnection Condition and the Self-Organization of Solar Coronal Heating, *Astrophys. J.*, *671*, 2139–2153.
- Vaivads, A., M. André, S. C. Buchert, J.-E. Wahlund, A. N. Fazakerley, N. Cornilleau-Wehrin (2004), Cluster observations of lower hybrid turbulence within thin layers at the magnetopause, *Geophys. Res. Lett.*, *31*, CiteID L03804.
- Vaivads, A., A. Retinò, and M. André (2006), Microphysics of Magnetic Reconnection, *Space Sci. Rev.*, *122*, 19–27.
- Vasyliunas, V. M. (1975), Theoretical models of magnetic field line merging, *I. Rev. Geophys. Space Phys.*, *13*, 303–336.
- Wang, T., L. Sui, and J. Qiu (2007), Direct Observation of High-Speed Plasma Outflows Produced by Magnetic Reconnection in Solar Impulsive Events, *Astrophys. J.*, *661*, L207–L210.
- Wang, Y.-M., N. R. Sheeley, Jr., D. G. Socker, R. A. Howard, and N. B. Rih (2000), The dynamical nature of coronal streamers, *J. Geophys. Res.*, *105*, 25133–25142.
- Webb, D. F., J. Burkepile, T. G. Forbes, and P. Riley (2003), Observational evidence of new current sheets trailing coronal mass ejections, *J. Geophys. Res.*, *108*, SSH 6-1, CiteID 1440, DOI 10.1029/2003JA009923.
- Wood, P., and T. Neukirch (2005), Electron Acceleration in Reconnecting Current Sheets, *Sol. Phys.* *226*, 73–95.
- Wu, S. T., A.-H. Wang, S. P. Plunkett, and D. J. Michels, (2000), Evolution of Global-Scale Coronal Magnetic Field due to Magnetic Reconnection: The Formation of the Observed Blob Motion in the Coronal Streamer Belt, *Astrophys. J.*, *545*, 1101–1115.
- Xiao, C. J., Z. Y. Pu, X. G. Wang, Z. W. Ma, S. Y. Fu, and another 9 co-authors (2007), A Cluster measurement of fast magnetic reconnection in the magnetotail, *Geophys. Res. Lett.*, *34*, CiteID L01101.
- Yang, W.-H., and R. W. Schunk (1989), Discrete events and solar wind energization, *Astrophys. J.*, *343*, 494–498.
- Yokoyama, T., K. Akita, T. Morimoto, K. Inoue, and J. Newmark (2001), *Astrophys. J.*, *546*, L69–L72.
- Yokoyama, T., and K. Shibata (1996), Numerical Simulation of Solar Coronal X-Ray Jets Based on the Magnetic Reconnection Model, *Publ. Astron. Soc. Japan* *48*, 353–376.

J. Lin, National Astronomical Observatories of China/Yunnan Astronomical Observatory, Chinese Academy of Sciences, Kunming, Yunnan 650011, China & Harvard-Smithsonian Center for Astrophysics, 60 Garden Street, Cambridge, MA 02138, USA. (jlin@ynao.ac.cn)

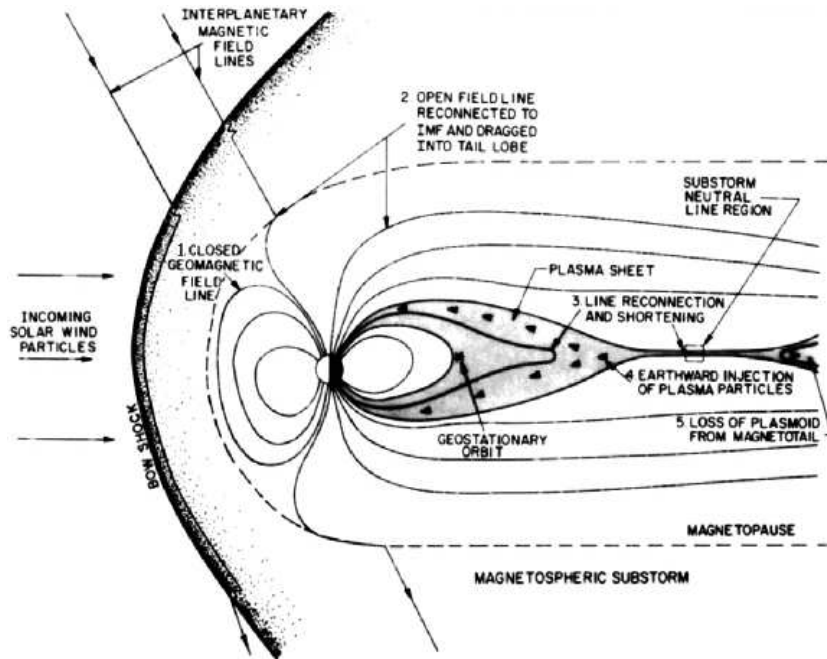


Figure 1. Schematic diagram of magnetic reconnection processes occurring in the magnetosphere. Interplanetary magnetic field in the solar wind reconnect with the terrestrial field near the front of the magnetosphere (stage 1) and are dragged back to form the tail lobes, sending plasma and magnetic energy there and forming the neutral plasma (current) sheet (stage 2). When the sheet becomes thin enough as a result of the increase in the magnetic pressure in the lobes, magnetic reconnection commences and releases the magnetic energy to heat and accelerate magnetotail plasma (stage 3), sending plasmoids towards (stage 4) and away from the Earth (Stage 5). From Figure 1 of *Baker et al.* [1987].

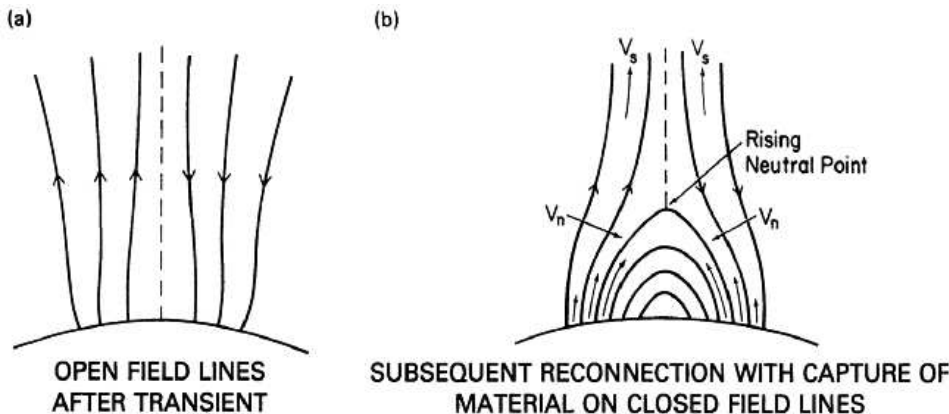


Figure 2. The two-ribbon flare model by *Kopp and Pneuman* [1976]. (a) The magnetic field is pushed open by an eruption and a current sheet separates two anti-parallel magnetic field lines. (b) The opened configuration relaxes into a closed, nearly potential field via magnetic reconnection in the current sheet. This process produces two bright and separating flare ribbons on the solar disk, and a continually growing flare loop system in the corona. From *Kopp and Pneuman* [1976].

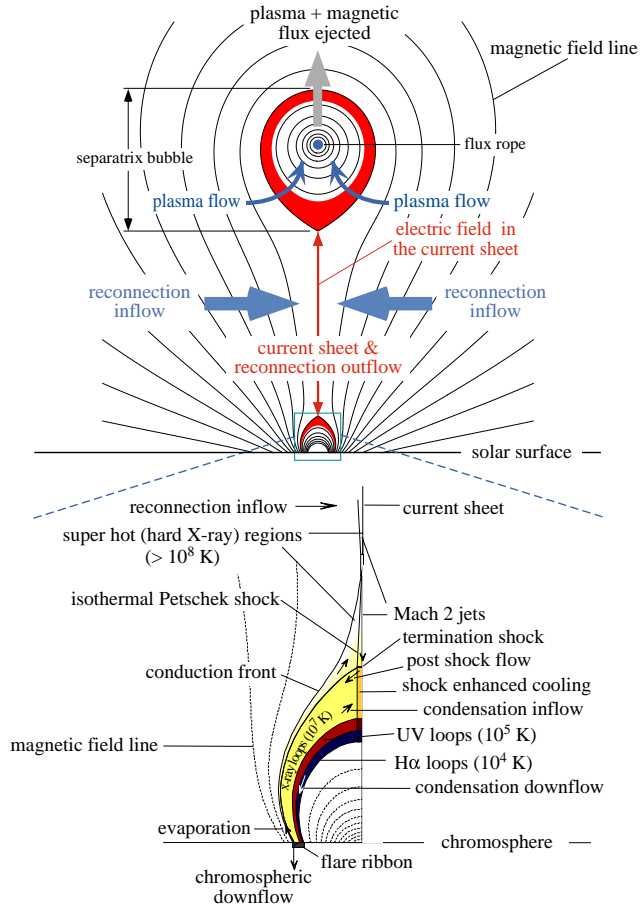


Figure 3. Schematic diagram of a disrupted magnetic field that forms in an eruptive process. Colors are used to roughly denote the plasma layers in different temperatures. This diagram incorporates the two-ribbon flare configuration of *Forbes and Acton* [1996] and the CME configuration of *Lin and Forbes* [2000], and provides a comprehensive description of how various manifestations in the solar eruption are related to one another. The morphological features of the disrupting magnetic field in the event studied by *Lin et al.* [2005] nearly duplicated those of this diagram (cf. Figure 5 of *Lin et al.* [2005]).

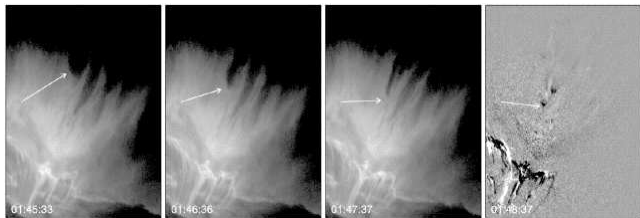


Figure 4. *TRACE* 195 Å filtergrams of the 2002 April 21 west-limb flare showing Fe XII postflare loops (lower left) and the Fe XXIV plasma cloud (center) penetrated by dark tadpole-like inflows (upper right). The fourth panel is a difference image showing the change between the images at 0147 and 0148 UT. These images have been rotated so that the solar limb is approximately horizontal. The arrow refers to a “tadpole” flowing toward to the Sun. The vertical dimension of each panel is approximately 1.17×10^5 km. From *Sheeley et al.* [2004].

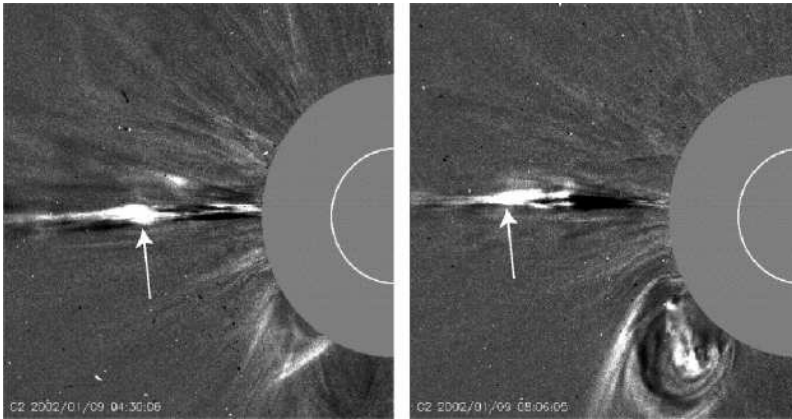


Figure 5. Running difference images of two examples of the plasma blobs observed by LASCO C2 flowing away from the Sun along the current sheet. From *Ko et al.* [2003].

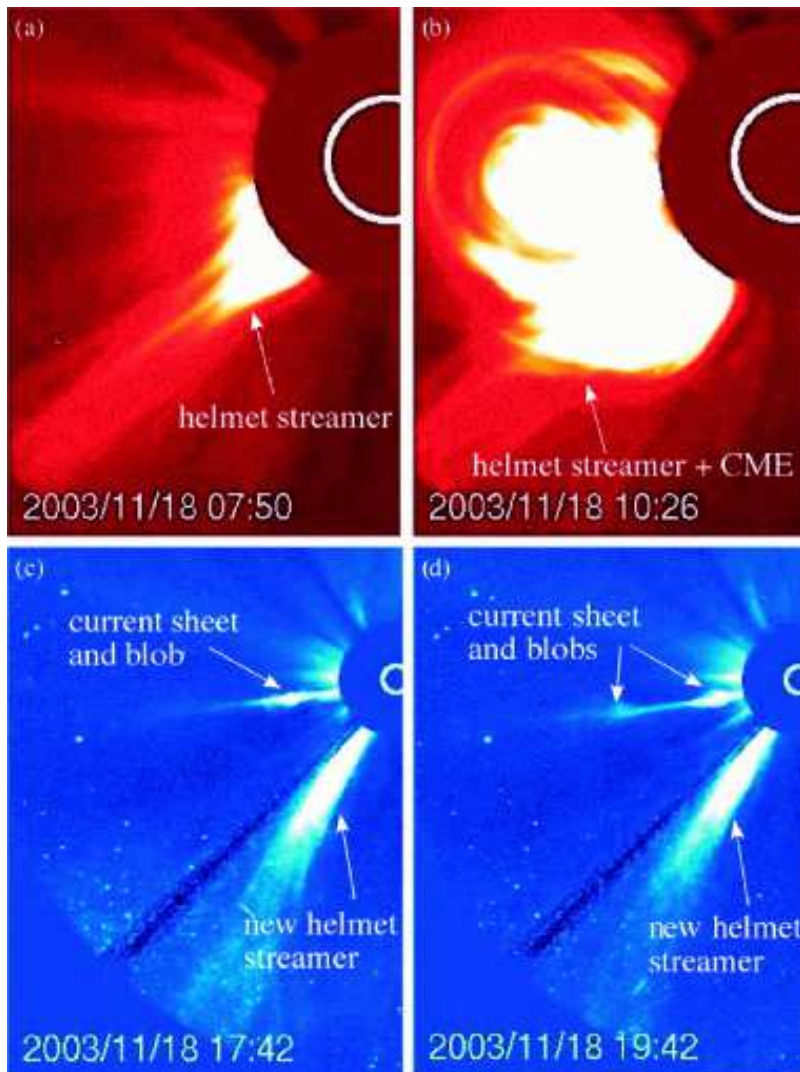


Figure 6. A fast CME was observed by LASCO C2 (panels a and b), and a long thin current sheet left behind by the CME can be seen in LASCO C3 images with two well recognized plasma blobs flowing away from the Sun (panels c and d). From *Lin et al.* [2005].

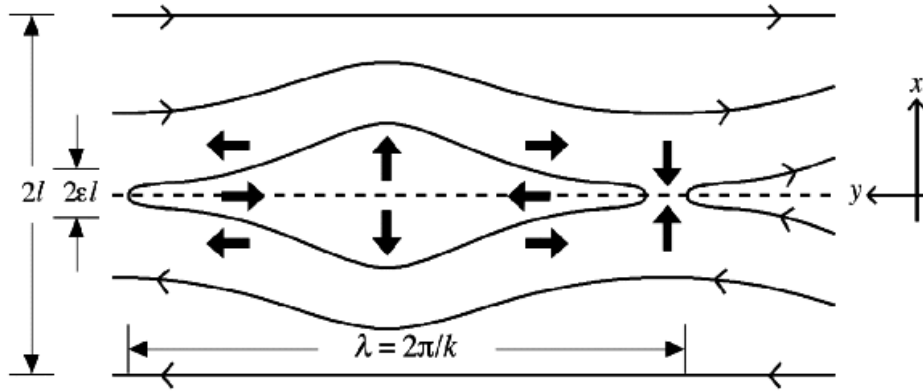


Figure 7. Interior structure of the current sheet in which the tearing mode instability develops. Thick arrows show plasma flow and thin arrows are for magnetic field lines. (Courtesy of E. R. Priest.)

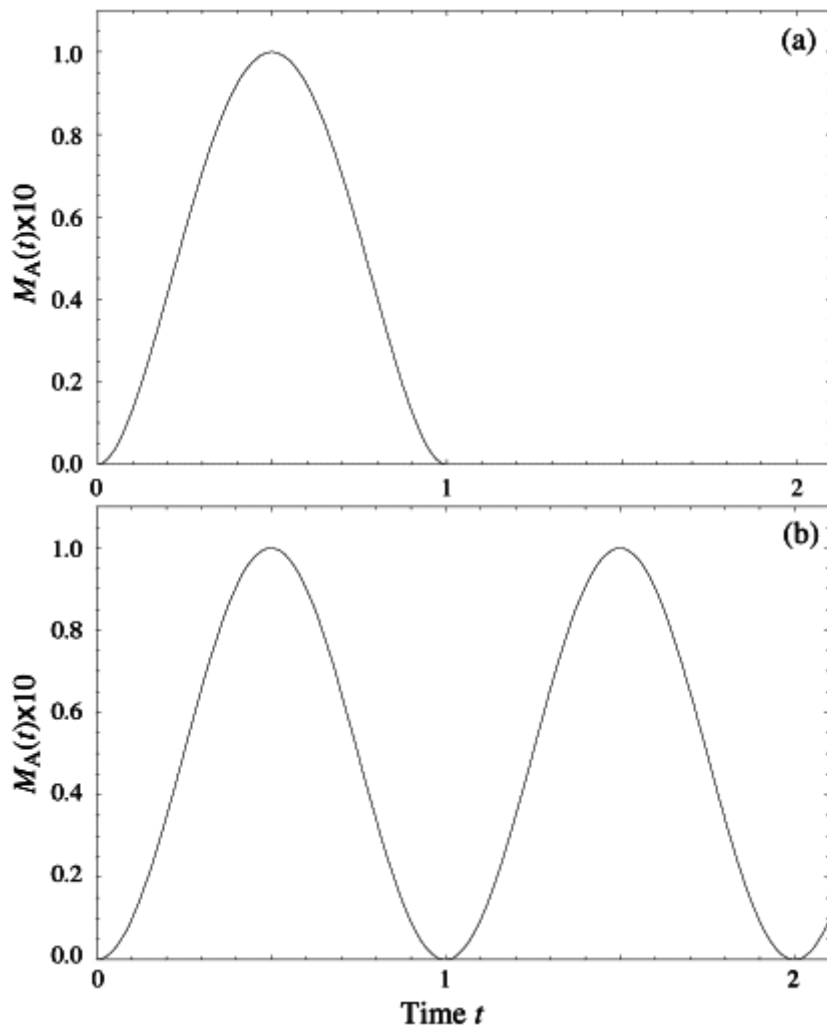


Figure 8. Variations of $M_A(t)$ versus time. (a) Single pulse reconnection governed by (6), and (b) bursty reconnection described by (7)

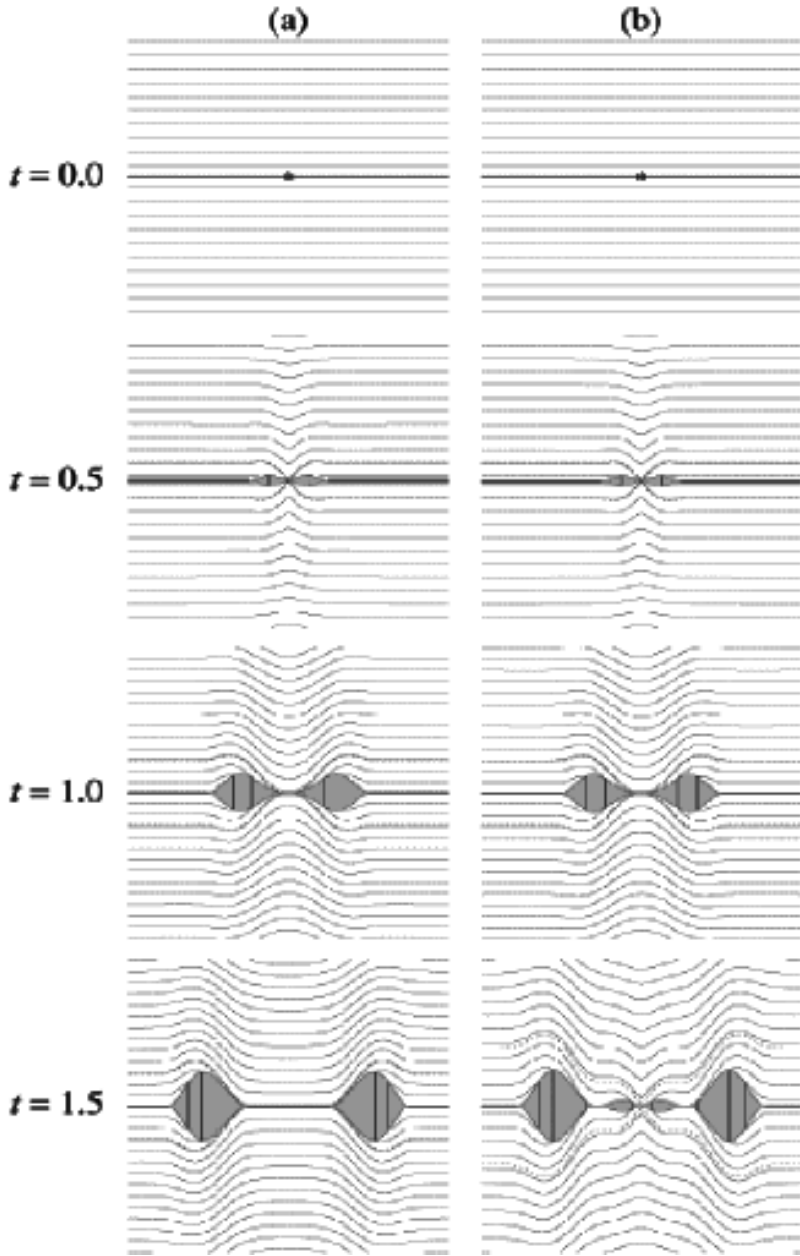


Figure 9. Evolution of the hydromagnetic configurations in the time-dependent Petschek-type reconnection in response to the single pulse dissipation (a), and to the bursty dissipation (b), respectively. Panels are for the snapshots of the hydromagnetic configurations at different times. The asterisks in the panels for $t = 0$ indicate the location where reconnection is initiated, solid curves describe magnetic field lines, thick solid lines are for the current sheets, dashed curves manifest the separatrices, and the shadowed areas are the reconnection outflow regions surrounded by the slow mode shocks. The x -axis points to the right, the y -axis points upward, and the origin is co-located with the asterisk. The scale in y -direction in each panel has been enlarged by a factor of 10 in order to display detailed structures of the disturbance.

Table 1. Some important parameters for plasmas in various circumstances

	B^a		n_e (cm^{-3})		V_A (10^3 km s^{-1})		β^b	
Sun ^c	AR 10^2	Ph 10^3	AR 10^{10}	Ph 10^{17}	AR 1	Ph < 0.01	AR 3.5×10^{-3}	Ph > 2
Earth	Dayside ^d 100 NECPS ^f 5	Tail lobe ^e 20 MDPS ^g 5	Dayside 100 NECPS 0.35	Tail lobe 0.01 MDPS 0.25	Dayside 0.22 NECPS 0.78	Tail lobe 4.4 MDPS 0.16	Dayside 0.34 NECPS 25	Tail lobe 8.6×10^{-3} MDPS 1

^a Units of magnetic field strength in the corona is G, and that in the magnetosphere is nT.

^b Plasma β , the ratio of the gas pressure to the magnetic pressure, $8\pi n_e kT/B^2$. Here temperature $T = 10^6$ K in the corona and in the magnetopause, and k is the Boltzmann constant.

^c Parameters for the solar atmosphere. AR indicates the coronal base over the active region, and Ph stands for the photosphere.

^d Parameters are measured at about 10 Earth radii close to the noon direction. (e.g., see also *Paschmann et al.* [1986]).

^e For comparison with solar flares, near tail (around $20 R_E$ or so) data are used here: $B = 20$ nT, $T = 10^7$, and $n_e = 0.01 \text{ cm}^{-3}$.

^f Information from statistical survey by AMPTE/IRM in 1986 of ion/proton moments in the near-Earth (between -9 and -18 R_E of GSM distance) central plasma sheet (NECPS) [*Baumjohann et al.* 1989]. Note: What *Baumjohann et al.* [1989] used was the ion density. So by quoting this as n_e we are assuming an electron-proton population and charge neutrality. A typical ion temperature in NECPS is $T_i = 5 \times 10^7$ K, and the electron temperature is around $T_e = 10^7$ K.

^g Information for the middle distance plasma sheet (MDPS) from *Slavin et al.* [1985].